NASA TECHNICAL NOTE

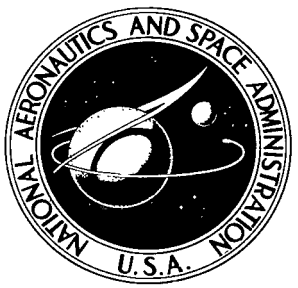

NASA TN D-6356

NASA TN D-6356

MOLECULAR DYNAMICS OF POLAR GAS ROTATIONAL RELAXATION

by Frank J. Zeleznik, John V. Dugan, Jr., and Raymond W. Palmer

Lewis Research Center
Cleveland, Ohio 44135

NATIONAL AERONAUTICS AND SPACE ADMINISTRATION • WASHINGTON, D. C. • JUNE 1971

1. Report No.	2. Government Accession No.	3. Recipient's Catalog No.
NASA TN D-6356		

4. Title and Subtitle
MOLECULAR DYNAMICS OF POLAR GAS ROTATIONAL RELAXATION

5. Report Date
June 1971

6. Performing Organization Code

7. Author(s)
Frank J. Zeleznik, John V. Dugan, Jr., and Raymond W. Palmer

8. Performing Organization Report No.
E-5852

9. Performing Organization Name and Address
Lewis Research Center
National Aeronautics and Space Administration
Cleveland, Ohio 44135

10. Work Unit No.
129-01

11. Contract or Grant No.

12. Sponsoring Agency Name and Address
National Aeronautics and Space Administration
Washington, D. C. 20546

13. Type of Report and Period Covered
Technical Note

14. Sponsoring Agency Code

15. Supplementary Notes

16. Abstract
A 50-molecule sample in contact with a heat bath of similar molecules is used as a model to calculate the rotational collision numbers Z_{rot} for HCl and DCl at 300 and 500 K, by the method of molecular dynamics. The mean rotational energy of the sample exhibits an exponential approach to a steady-state value; however, there is considerable scatter about the exponential curve. The results for Z_{rot} generally agree with previous theoretical calculations and these results are intermediate to both experimental acoustic data and the earlier perturbation results.

17. Key Words (Suggested by Author(s))	18. Distribution Statement
	Unclassified - unlimited

19. Security Classif. (of this report)	20. Security Classif. (of this page)	21. No. of Pages	22. Price*
Unclassified	Unclassified	47	$3.00

*For sale by the National Technical Information Service, Springfield, Virginia 22151

MOLECULAR DYNAMICS OF POLAR GAS ROTATIONAL RELAXATION

by Frank J. Zeleznik, John V. Dugan, Jr., and Raymond W. Palmer

Lewis Research Center

SUMMARY

A 50-molecule sample in contact with a heat bath of similar molecules was used as a model to calculate the rotational collision numbers Z_{rot} for HCl and DCl at 300 and 500 K, by the method of molecular dynamics. The mean rotational energy of the sample exhibits an exponential approach to a steady-state value; however, there was considerable scatter about the exponential curve. The results for Z_{rot} generally agree with previous theoretical calculations and these results are intermediate to both experimental acoustic data and the earlier perturbation results.

INTRODUCTION

Accurate experimental studies of relaxation phenomena on the macroscopic level are difficult at best. This difficulty is compounded by the existence of two different theoretical definitions of a relaxation time and, furthermore, these definitions are generally used interchangeably. Previous papers (refs. 1 and 2) applied these two definitions to the special case of rotational relaxation in polar gases. Both of these papers were essentially analytical calculations and were motivated by the desire to obtain a closed-form expression for the rotational collision number Z_{rot} arising from each definition. In both cases a classical perturbation calculation was carried out through third order. Reference 1 used the energy relaxation definition of a relaxation time, while reference 2 employed the definition based on volume viscosity.

The results of references 1 and 2 can be succinctly stated in the following manner:

(1) The two definitions agree exactly through third order in perturbation (apart from a multiplicative adjustable parameter).

(2) Theoretically calculated values of Z_{rot} increase for either a decrease in the dipole moment or a decrease in the moment of inertia; generally speaking, Z_{rot} increases with temperature, but in some cases it may exhibit a shallow minimum.

(3) The extraction of experimental rotational relaxation times from polar gas thermal conductivity measurements is highly suspect.

These conclusions can only be given tentative acceptance since they are based on a calculation which was not only a perturbation calculation but also was restricted to a two-dimensional model.

The present report examines the effect of both the perturbation calculation and the two-dimensional model vis-à-vis the energy relaxation definition of a relaxation time. All the results are for a three-dimensional model of a polar gas whose rigid-rod molecules interact by means of spherical hard cores with embedded point dipoles aligned along the symmetry axis. Further, all calculations are carried out numerically to avoid the perturbation assumption. The molecular dynamics approach to studying rotational relaxation in polar gases is used.

Generally, the method of molecular dynamics is applied to dense fluids or solids to study both their time-dependent and time-independent properties. For example, Rahman (refs. 3 and 4) studied liquid argon by this technique and calculated the pair-correlation function, the self-diffusion coefficient, the velocity auto-correlation function, and the time-dependent pair-correlation function. Similarly, Verlet (refs. 5 and 6) calculated the temperature, pressure, internal energy, and the pair-correlation function and its Fourier transform for liquid argon. In these cases the system "thermalized" quite rapidly and required on the order of 2×10^{-12} seconds to reach equilibrium (refs. 5 and 7). Köhler, Bellemans, and Gancberg (refs. 8 and 9) studied a system of weakly interacting electric dipoles confined to a rigid, square lattice. They examined the approach to equilibrium for such a system in terms of the first, second, and fourth moments of angular momentum and Boltzmann's H-function - the second moment being essentially the kinetic energy. They experienced difficulties in extracting relaxation times because of large fluctuations. An interesting aspect of this work is the demonstration of the existence of a set of initial conditions for which the system does not exhibit a definite temporal evolution. This is similar to the situations observed by Hirooka and Saito (ref. 10) in their study of a two-dimensional square lattice of coupled anharmonic oscillators. They demonstrated the existence of an induction period that preceded the evolution toward equilibrium. For a sufficiently weak coupling of the oscillators they could not detect any appreciable approach to equilibrium.

All the examples of the molecular dynamics approach discussed to this point were similar in the sense that a macroscopic system was approximated by a finite system. The classical equations of motion for this finite system were then solved numerically. Such a procedure is necessary for liquids and solids because of the high densities involved. For low-density gases, on the other hand, the binary collision approximation can be invoked. This permits the decoupling of the large set of equations describing the evolution of the model into smaller subsets, with each subset now describing the interaction of a pair of molecules. It is possible to simplify the procedure even further by

introducing the idea of a heat bath, an infinitely large system that always remains in equilibrium. If a small sample system is immersed in the heat bath, all interactions among members of the small system may be ignored and only interactions between the heat bath and the sample system need be considered. A model of this kind has been used to study the relaxation of diatomic molecules in a heat bath by Alterman and Wilson (ref. 11), Raff (ref. 12), and Berend and Benson (ref. 13).

Alterman and Wilson studied the vibrational relaxation of 50 bromine molecules in a heat bath of xenon atoms. They terminated their calculations after fewer than 250 collinear collisions between the molecules and atoms. A vibrational relaxation time was obtained from the initial slope of the mean vibrational energy of the 50 molecules as a function of the number of collisions. It was not possible for them to determine relaxation times from all the calculations since in some cases there was no obvious choice of an initial slope.

The rotational relaxation calculations of Raff (ref. 12) and Berend and Benson (ref. 13) are similar in gross features; however, they differ considerably in their fine structure. Both calculated a relaxation time in terms of a mean rate of energy transfer which effectively plays the same role as the initial slope in the Alterman and Wilson (ref. 11) calculations. However, Raff used a three-dimensional average calculated over a three-dimensional flux distribution, while Berend and Benson performed a two-dimensional calculation and averaged over a two-dimensional Boltzmann distribution. In view of these differences it is not surprising to find that their results do not agree when both calculate a common system. Thus, Raff's calculations are lower by a factor of 5, while Berend and Benson's calculations are higher by about the same amount when compared to the acoustic data of Jonkman and Ertas (ref. 14) for the rotational relaxation of p-H_2 by He.

The calculations described in this report are more akin to those of Alterman and Wilson (ref. 11) than they are to those of Raff (ref. 12) and Berend and Benson (ref. 13), in the sense that we follow the relaxation of a polar gas coupled to a heat bath. However, in contrast to the one-dimensional treatment of Alterman and Wilson, we shall carry out a three-dimensional calculation for a sufficient number of collisions to assess whether or not there is an exponential approach to equilibrium. Also we shall try to extract rotational collision numbers as well as their dependence on the temperature, dipole moment, and moment of inertia. Specifically, a relatively small sample containing N molecules is placed into a heat bath of the same kind of molecules. An observation of the rotational energy of the sample as a function of the number of collisions n between the sample and heat bath molecules should enable us to determine the rate at which the sample approaches an equilibrium with the heat bath. If the sample approaches equilibrium exponentially, we should be able to extract a relaxation time from the data, provided that the sample and the heat bath are always in translational equilibrium but are not initially in rotational equilibrium. The rotational relaxation time τ_R for such a situation is defined by

$$\frac{dE_R}{dt} = -\frac{E_R - E_\infty}{N\tau_R} \tag{1}$$

where E_R is the rotational energy per particle of the sample and $E_R(t = \infty) = E_\infty$. If $E_R(t = 0) = E_0$, integration of equation (1) gives

$$E_R - E_0 = (E_\infty - E_0)\left(1 - e^{-t/\tau_R N}\right) \tag{2}$$

If the mean time between collisions is denoted by τ_c, then the number of collisions n and the rotational collision number Z_{rot} are defined by

$$n = \frac{t}{\tau_c}$$

$$Z_{rot} = \frac{\tau_R}{\tau_c} \tag{3}$$

Combining equations (2) and (3) produces

$$E_R - E_0 = (E_\infty - E_0)\left[1 - \exp\left(-\frac{n}{NZ_{rot}}\right)\right] \tag{4}$$

Expression (4) can be used to extract rotational collision numbers from the variations of E_R with n.

ANALYSIS OF THE CALCULATION

The numerical experiment which we shall carry out is conceptually quite simple, but its interpretation is far from simple. To see this, consider an ensemble of such experiments; that is, we construct a very large number of identical replicas of the N-molecule sample system. Each of these replicas is observed as its rotational energy evolves when it is placed into contact with a heat bath for a fixed time period (or a fixed number of collisions). Because of the random nature of the interaction between the sample and the heat bath and because of the finite sample size, it is unrealistic to expect either that the evolution of E_R will be a smooth exponential or that all members of the ensemble will evolve along a common curve. Thus our ensemble of experiments generates an ensemble of curves and each curve exhibits many fluctuations or changes in slope.

No one member of the ensemble of numerically generated "experimental" curves adequately describes the real physical situation; however, it is reasonable to expect that an ensemble average of the data would be physically relevant and could be used to extract a Z_{rot} (see top half of fig. 1). Further, the fluctuations in the data for one member of the ensemble about the mean of the ensemble data are minimized by a sufficiently large sample size N. Hence, the ideal, but economically unfeasible, numerical experiment would be to observe an ensemble of samples, each sample consisting of very many molecules, for a very long period of time. By contrast, the practical calculation would be to observe one member of an ensemble of samples, each sample consisting of a few molecules, for a relatively short period of time. Considerations of computation time alone require that N be about 50, certainly not much larger. The length of time that a sample must be observed in order to adequately characterize its temporal evolution is certainly open to question. Obviously, the observational period must be considerably longer than the periods of the fluctuations in the curve. Intuitively, it seems reasonable to require that the observational period at least satisfy the inequality $n > NZ_{rot}$.

Let us now assume that we have observed, for a relatively short period, the evolution of E_R for one sample of size N. How is this data to be analyzed, in terms of equation (4), in order to obtain a physically relevant Z_{rot}? We can either regard equation (4) as containing two fitting parameters Z_{rot} and E_∞, or else we can fix E_∞ at the value corresponding to the equilibrium rotational energy E_{eq} and use only Z_{rot} as a fitting parameter. Presumably, the two methods would give the same result for Z_{rot} when applied to the ensemble data of the ideal experiment discussed previously. It is, however, unlikely that they will give the same results for Z_{rot} when applied to the practical calculation. It is not possible to say which method will give the more physically realistic result, although the two-parameter method will certainly give the best possible representation of the temporal evolution of E_R. For this reason both the two-parameter and one-parameter methods are used to analyze the data. Within either the two-parameter or one-parameter framework we must still attempt to obtain a Z_{rot} from the data of one member of the ensemble which might be comparable to that determined by the data of the entire ensemble. For this reason a heuristic alternative to the analysis of the ensemble data is described. The description is given in terms of the two-parameter treatment of the data, but it is equally applicable to the one-parameter treatment.

The random nature of the interaction between the heat bath and the sample has been previously pointed out. Thus, if equation (4) were fitted to the data of each ensemble member separately, a somewhat different pair of "best" parameters would be obtained, reflecting the different history of each replica (see bottom half of fig. 1). In effect, the parameters Z_{rot} and E_∞, which characterize the evolution of the replica during the short observational period, are random variables. In principle, it should be possible to construct new random variables from Z_{rot} and E_∞ which will serve as unbiased

estimators of the physically relevant Z_{rot} and E_{eq} which would be obtained from an analysis of the data of the entire ensemble.

Now observe that the duration of observation simply cannot remove the randomness of the heat bath - sample interaction. Suppose then that a given member of the ensemble has been observed for a sufficiently large number of collisions $n_1 > NZ_{rot}$ and the data analyzed to extract the two parameters $Z_{rot}(1)$ and $E_{\infty}(1)$. This sample is allowed to continue its evolution until there have been an additional Δn collisions and then the parameters $Z_{rot}(2)$ and $E_{\infty}(2)$ are obtained. Proceeding in this fashion, $Z_{rot}(k)$ and $E_{\infty}(k)$ are obtained at $n_k = n_{k-1} + \Delta n$ collisions. Each fixed increment Δn is a random increment in the random history of the sample and, therefore, it appears plausible to approximate the ensemble average Z_{rot} by the mean of $Z_{rot}(k)$

$$\left(Z_{rot}\right)_{physical} \approx \frac{1}{k_{max}} \sum_{k=1}^{k_{max}} Z_{rot}(k)$$

The value of k_{max} is determined largely by what is considered to be an economically acceptable amount of computation.

The mean of the values of $E_{\infty}(k)$ can be used in an attempt to justify the termination of the calculation, a posteriori, in the following manner: It is well known that the mean of a random sample of size N drawn from some distribution is not, in general, equal to the first moment of the distribution. Instead, a set of such means is distributed about the first moment. It might be expected that the mean values of E_{∞} from calculations done at different conditions would exhibit variations about E_{eq} comparable to those obtained in drawing a random sample of size N from an equilibrium distribution. On this basis, then, if the distribution of the mean values of E_{∞} is radically different from that expected of random samples of size N, we would suspect that an insufficient number of collisions had been studied. On the other hand, we could reasonably hope that if the distribution of mean values of E_{∞} is consistent with that expected of a sample of size N, then enough collisions had been studied. For this purpose we must know the probability that a sample of size N, when drawn from an equilibrium distribution, will have a rotational energy within a given interval about the population mean.

Consider the equilibrium distribution of molecular rotational energy ϵ. If the molecule possesses two degrees of freedom, the distribution function at a temperature T is given by

$$f(\epsilon)d\epsilon = \beta e^{-\beta\epsilon}\, d\epsilon \qquad 0 \leq \epsilon \leq \infty \tag{5}$$

where $\beta^{-1} = kT$ and k is Boltzmann's constant. This is an example of a χ^2-distribution with ν degrees of freedom

$$f(\chi^2)d(\chi^2) = \frac{1}{2\Gamma\left(\frac{\nu}{2}\right)}\left(\frac{\chi^2}{2}\right)^{(\nu/2)-1} e^{-\chi^2/2}d(\chi^2) \tag{6}$$

where ν has been set equal to 2. This can be easily seen by making a change of variables $\chi^2 = 2\beta\epsilon$ in equation (5). The moment-generating function for equation (6) is given by

$$M_{\chi^2}(\theta) \equiv \int_0^\infty e^{\theta\chi^2} f(\chi^2)d(\chi^2) = (1 - 2\theta)^{-\nu/2} \tag{7}$$

Instead of considering the distribution of E_R

$$E_R = \frac{1}{N}\sum_{i=1}^{N} \epsilon_i \tag{8}$$

it is convenient to consider the distribution of the dimensionless quantity βE_R.

$$\beta E_R = \frac{1}{N}\sum_{i=1}^{N} \beta\epsilon_i \tag{9}$$

From the properties of the moment-generating function (ref. 15, p. 135), it follows that

$$M_{\beta E_R}(\theta) \equiv \int_0^\infty e^{\beta E_R \theta} F(\beta E_R)d(\beta E_R) = \left[M_{\beta\epsilon}\left(\frac{\theta}{N}\right)\right]^N \tag{10}$$

where F is the distribution function for βE_R. But using the transformation $\chi^2 = 2\beta\epsilon$, as before, $M_{\beta\epsilon}(\theta)$ can be expressed in terms of $M_{\chi^2}(\theta)$.

$$M_{\beta\epsilon}(\theta) = M_{\chi^2/2}(\theta) = M_{\chi^2}\left(\frac{\theta}{2}\right) \tag{11}$$

Hence, combining equations (7) and (11) with equation (10),

$$M_{\beta E_R}(\theta) = \left(1 - \frac{\theta}{N}\right)^{-N\nu/2}$$

where ν should actually be set equal to 2 Thus, βE_R is also distributed as a χ^2-distribution but with $N\nu/2$ degrees of freedom In fact, it can be verified that βE_R has the distribution

$$F(\beta E_R)d(\beta E_R) = \frac{N}{\Gamma\left(\frac{N\nu}{2}\right)}\left(N\beta E_R\right)^{(N\nu/2)-1} \exp\left(-N\beta E_R\right)d(\beta E_R) \tag{13}$$

The moments of this distribution are

$$\mu_n \equiv \frac{d^n}{d\theta^n} M_{\beta E_R}(\theta)\bigg|_{\theta=0} = N^{-n}\left(\frac{N\nu}{2}\right)\left(\frac{N\nu}{2}+1\right)\ldots\left(\frac{N\nu}{2}+n-1\right) \tag{14}$$

while its cumulants are

$$\kappa_n \equiv \frac{d^n}{d\theta^n} \ln M_{\beta E_R}(\theta)\bigg|_{\theta=0} = \frac{\nu}{2} N^{1-n}(n-1)! \tag{15}$$

Note that, for large N, βE_R is a normal variable, with $\mu_1/\sqrt{\kappa_2} = \sqrt{N\nu/2}$.

Now the probability P that a random sample of size N will have a βE_R that lies in the interval $(1 \pm p)\mu_1$ about the mean μ_1 can easily be calculated. Here p satisfies the condition $0 < p \leq 1$.

$$P\left(\frac{N\nu}{2}, p\right) = \int_{(1-p)\mu_1}^{(1+p)\mu_1} F(\beta E_R)d(\beta E_R) = \frac{1}{\Gamma\left(\frac{N\nu}{2}\right)}\int_{N\nu(1-p)/2}^{N\nu(1+p)/2} z^{(N\nu/2)-1}e^{-z}\,dz \tag{16}$$

The probability P can be readily evaluated in terms of the incomplete Γ-function ratio

$$I(u,q) \equiv \frac{1}{\Gamma(q+1)}\int_0^{u\sqrt{q+1}} v^q e^{-v}\,dv$$

which has been tabulated by Harter (ref 16).

$$P\left(\frac{N\nu}{2}, p\right) = I\left[(1+p)\left(\frac{N\nu}{2}\right)^{1/2}, \frac{N\nu}{2} - 1\right] - I\left[(1-p)\left(\frac{N\nu}{2}\right)^{1/2}, \frac{N\nu}{2} - 1\right] \tag{17}$$

Figure 2 is a plot of P as a function of $N\nu/2$, with p taken as a parameter. It is apparent from this figure that the one-parameter family of curves grows quite slowly beyond $N\nu/2 = 50$. Since ν equals 2 for the rotational energy distribution, the sample size N would have to be quite large for the sample means to be sharply clustered about the first moment. Since N has been chosen equal to 50, there should be substantial fluctuations in the mean values of E_∞.

CALCULATION METHOD

The calculational method has been described in general terms. Some of the specifics are presented in this section. The physical system is a gas composed of polar molecules which are represented as rigid rods surrounded by a spherical hard cores with embedded point dipoles. The rotational energies of a sample of $N = 50$ such molecules is distributed randomly over a χ^2-distribution with $\nu = 2$ degrees of freedom and a temperature of $T = T_0$. The translational velocities of these molecules are assumed to be in equilibrium with a heat bath of the same molecules and are characterized by a Boltzmann distribution at a temperature $T > T_0$. Thus, it is not necessary to keep track of the translational energies of the sample molecules during the computation. The calculation is carried out by performing the following steps repetitively:

(1) One "sample" molecule and one "heat bath" molecule are randomly selected as collision partners.

(2) The two molecules scatter and, in so doing, alter the rotational energy of the "sample molecule."

(3) After each scattering, a new mean rotational energy of the sample molecules is computed.

The details of random selection are given in the following section; the balance of this section is devoted to a discussion of the scattering equations of motion and their numerical solution.

The relative motion of two molecules is described by the Lagrangian equations obtained from the Lagrangian

$$L = T_{trans} + T_{rot}(1) + T_{rot}(2) - V - \Phi_c \tag{18}$$

where T_{trans} is the kinetic energy of relative motion, $T_{rot}(i)$ (where $i = 1,2$) is the rotational kinetic energy of the i^{th} molecule, V is the dipole-dipole interaction, and Φ_c is a spherical hard-core potential of diameter $\sigma = (\sigma_1 + \sigma_2)/2$ (where σ_1 and σ_2 are the molecular diameters of the colliding molecules). The rotational kinetic energy is conventionally written in terms of the Euler angles (ref. 17). However, since we are dealing with rigid rods, only two angles are needed to specify the orientation and these might just as well be chosen as the spherical angles θ and ϕ (where θ is the polar angle and ϕ the azimuthal angle). Hence,

$$T_{rot}(j) = I_j \frac{\left(\dot{\theta}_j^2 + \dot{\phi}_j^2 \sin^2\theta_j\right)}{2} \qquad j = 1,2 \tag{19}$$

This form possesses the distinct disadvantage that it leads to the appearance of $\sin\theta_j$ in the denominator of the differential equation determining ϕ_j, resulting in undesirable numerical consequences when θ_j is near either zero or π. This difficulty can be easily circumvented by describing the rotational motion of a rigid rod in terms of Cartesian coordinates $\vec{x}_j$ (where $j = 1,2$) and by constraining these coordinates to lie on a unit sphere (ref. 18). The angles θ_j and ϕ_j now describe the orientation of the unit vectors $\vec{x}_j$.

The foregoing considerations lead to

$$T_{rot}(j) = \frac{I_j \dot{\vec{x}}_j \cdot \dot{\vec{x}}_j}{2} \qquad j = 1,2 \tag{20}$$

subject to the constraints

$$\eta_j(x_j) \equiv \frac{1}{2}\left(\vec{x}_j \cdot \vec{x}_j - 1\right) = 0 \qquad j = 1,2 \tag{21}$$

The factor 1/2 in equation (21) was inserted simply for later convenience. If $\vec{R} = (X,Y,Z)$ is the separation vector for the two molecules and m their reduced mass, the relative translational kinetic energy is

$$T_{trans} = m \frac{\dot{\vec{R}} \cdot \dot{\vec{R}}}{2} \tag{22}$$

while the dipole-dipole interaction has the form

$$V = \frac{\mu_1 \mu_2}{(\vec{R}\cdot\vec{R})^{3/2}}\left[\vec{x}_1\cdot\vec{x}_2 - \frac{3(\vec{x}_1\cdot\vec{R})(\vec{x}_2\cdot\vec{R})}{(\vec{R}\cdot\vec{R})}\right] \tag{23}$$

In this section μ_1 and μ_2 are the molecular dipole moments and do not designate moments of a distribution. Note that we have assumed that the dipole moment lies along the rigid rod. To incorporate the constraints it is convenient to define a new Lagrangian containing undetermined multipliers λ_j (where $j = 1, 2$) by

$$\mathcal{L} \equiv L + \lambda_1\eta_1 + \lambda_2\eta_2$$

and to consider the variational principle

$$\delta\int_{t_1}^{t_2}\mathcal{L}\,dt = 0 \tag{25}$$

In the variation of this integral, $\vec{R}$, $\vec{x}_j$, and λ_j are treated as independent and the variations in $\vec{R}$ and $\vec{x}_j$ are required to vanish at the end points. This is just a special case of the problem of Lagrange in the calculus of variations (refs. 19 and 20). Carrying out the required variations gives

$$\delta\int_{t_1}^{t_2}\mathcal{L}\,dt = \int_{t_1}^{t_2}\left[\frac{\partial L}{\partial\dot{\vec{R}}}\cdot\delta\dot{\vec{R}} + \frac{\partial L}{\partial\vec{R}}\cdot\delta\vec{R} + \sum_{i=1}^{2}\left(\frac{\partial L}{\partial\dot{\vec{x}}_i}\cdot\delta\dot{\vec{x}}_i + \frac{\partial L}{\partial\vec{x}_i}\cdot\delta\vec{x}_i + \lambda_i\frac{\partial\eta_i}{\partial\vec{x}_i}\cdot\delta\vec{x}_i + \eta_i\delta\lambda_i\right)\right]dt = 0$$

Using the fact that

$$\delta\dot{\vec{R}} = \frac{d}{dt}\,\delta\vec{R}$$

$$\delta\dot{\vec{x}}_j = \frac{d}{dt}\,\delta\vec{x}_j$$

and performing an integration by parts,

$$\delta \int_{t_1}^{t_2} \mathcal{L}\, dt = \left(\frac{\partial L}{\partial \dot{\vec{R}}} \cdot \delta \vec{R} + \sum_{i=1}^{2} \frac{\partial L}{\partial \dot{\vec{x}}_i} \cdot \delta \vec{x}_i \right) \Bigg|_{t=t_1}^{t=t_2}$$

$$+ \int_{t_1}^{t_2} dt \left(\left[\frac{\partial L}{\partial \vec{R}} - \frac{d}{dt} \left(\frac{\partial L}{\partial \dot{\vec{R}}} \right) \right] \cdot \delta \vec{R} + \sum_{i=1}^{2} \left\{ \left[\frac{\partial L}{\partial \vec{x}_i} - \frac{d}{dt} \left(\frac{\partial L}{\partial \dot{\vec{x}}_i} \right) + \lambda_i \frac{\partial \eta_i}{\partial \vec{x}_i} \right] \cdot \delta \vec{x}_i \right.\right.$$

$$\left.\left. + \eta_i \delta \lambda_i \right\} \right) = 0$$

The integrated terms disappear because the variations vanish at the end points. Thus the variations in R and x_j lead to the equations

$$\left.\begin{aligned} \frac{d}{dt} \left(\frac{\partial L}{\partial \dot{\vec{R}}} \right) - \frac{\partial L}{\partial \vec{R}} &= 0 \\ \frac{d}{dt} \left(\frac{\partial L}{\partial \dot{\vec{x}}_j} \right) - \frac{\partial L}{\partial \vec{x}_j} - \lambda_j \frac{\partial \eta_j}{\partial \vec{x}_j} &= 0 \qquad j = 1, 2 \end{aligned}\right\} \tag{26}$$

while the variations in λ_j give the constraint relations (eq. (21)).

The rather simple structure of the dipole-dipole interaction and the constraint relations makes it possible to avoid the explicit appearance of the multipliers in the equations of motion. Since $\partial \eta_j / \partial \vec{x}_j = \vec{x}_j$, it follows from the constraint relations (eq. (21)) that $\vec{x}_j \cdot (\partial \eta_j / \partial \vec{x}_j) = 1$. Equivalently, this follows from Euler's theorem on homogeneous functions. Hence, from the second member of equation (26)

$$\lambda_j = \vec{x}_j \cdot \left[\frac{d}{dt} \left(\frac{\partial L}{\partial \dot{\vec{x}}_j} \right) - \frac{\partial L}{\partial \vec{x}_j} \right] \tag{27}$$

The right side of this expression is rewritten by observing that $\partial L / \partial \vec{x}_j = -\partial V / \partial \vec{x}_j$, and since V is homogeneous of degree 1 in $\vec{x}_j$,

$$\vec{x}_j \cdot \frac{\partial L}{\partial \dot{\vec{x}}_j} = -V$$

where again Euler's theorem on homogeneous functions was used. Also since $\partial L/\partial \dot{\vec{x}}_j = I_j \dot{\vec{x}}_j$, and by twice differentiating the constraint equations (21) with respect to time to obtain $\vec{x}_j \cdot \ddot{\vec{x}}_j + \dot{\vec{x}}_j \cdot \dot{\vec{x}}_j = 0$, we find that

$$\vec{x}_j \cdot \frac{d}{dt}\left(\frac{\partial L}{\partial \dot{\vec{x}}_j}\right) = - I_j \dot{\vec{x}}_j \dot{\vec{x}}_j = -2T_{rot}(j) \tag{29}$$

Substituting equations (28) and (29) into equation (27) yields

$$\lambda_j = V - 2T_{rot}(j) \tag{30}$$

The complete set of working equations is now obtained by using equation (30) in equation (26), and adjoining equation (21) and its first derivative to the system to obtain

$$\left.\begin{aligned} M\ddot{\vec{R}} &= - \frac{\partial V}{\partial \vec{R}} \\ I_j \ddot{\vec{x}}_j &= \left[V - 2T_{rot}(j)\right] \vec{x}_j - \frac{\partial V}{\partial \vec{x}_j} \qquad j = 1, 2 \\ \vec{x}_j \cdot \vec{x}_j &= 1 \\ \vec{x}_j \cdot \dot{\vec{x}}_j &= 0 \end{aligned}\right\} \tag{31}$$

These equations are only applicable if $(\vec{R} \cdot \vec{R}) > \sigma^2$; when $(\vec{R} \cdot \vec{R}) = \sigma^2$, the molecules undergo a hard-sphere collision. The derivatives in equation (31) have the specific forms

$$\left.\begin{aligned} \frac{\partial V}{\partial \vec{R}} &= - \frac{3\mu_1\mu_2}{(\vec{R}\cdot\vec{R})^2}\left[(\vec{x}_1\cdot\vec{x}_2 - 5\vec{r}\cdot\vec{x}_1\vec{x}_2\cdot\vec{r})\vec{r} + \vec{r}\cdot\vec{x}_1\vec{x}_2 + \vec{x}_1\vec{x}_2\cdot\vec{r}\right] \\ \frac{\partial V}{\partial \vec{x}_1} &= \frac{\mu_1\mu_2}{(\vec{R}\cdot\vec{R})^{3/2}}(\vec{x}_2 - 3\vec{r}\vec{r}\cdot\vec{x}_2) \\ \frac{\partial V}{\partial \vec{x}_2} &= \frac{\mu_1\mu_2}{(\vec{R}\cdot\vec{R})^{3/2}}(\vec{x}_1 - 3\vec{r}\vec{r}\cdot\vec{x}_1) \end{aligned}\right\} \tag{32}$$

where $\vec{r} = \vec{R}/(\vec{R}\cdot\vec{R})^{1/2}$.

The equations of motion (eq. (31)) are solved numerically with a variable-step-size, fifth-order Runge-Kutta integration scheme. The method of altering the step size is described in appendix A. At each step of the integration the component of $\vec{x}_j$ with the largest absolute value is determined. Its value and the value of its time derivative at the end of the next step are calculated from the last two members of equation (31); concomitantly, the differential equation for this component is ignored. The remaining variables and their time derivatives are obtained from the differential equations contained in equation (31). The change in step size was determined by an empirical technique based on the error accumulated in the total energy of the pair of molecules. In all cases the total energy is conserved to better than about one part in 10^4. Random checks of time reversal showed that the coordinates returned to within several tenths of a percent of their initial values. The velocities were within a few percent of the initial values except for very few trajectories. The integration was terminated when the molecules were sufficiently separated so that the interaction potential was effectively negligible; that is, $\mu_1\mu_2/(\vec{R} \cdot \vec{R})^{3/2} \leq \min\left[T_{rot}(1), T_{rot}(2)\right]$. The average calculating time on an IBM 7094 was about 8 seconds per collision, although those trajectories characterized by low relative translational energies required considerably more computer time.

Each set of initial conditions for a potential collision was examined to determine whether the trajectory should be calculated. There were three circumstances under which a set of initial conditions was rejected. The first category of rejected initial conditions is that corresponding to collisions with projected running times in excess of 1 minute. A second class of rejected initial conditions is that corresponding to collisions with large impact parameters b. Such collisions can reasonably be expected to produce negligible changes in the rotational energy. These collisions were rejected if $b > 2.5\ \sigma$, where σ was the same for all molecules; this corresponds to impact parameters $b > 8.42$ Å. The third category of rejected initial conditions differs from the first two. The calculation of the trajectories in this category was attempted but had to be prematurely terminated because the integration step size became too small. The minimum allowable step size used was 10^{-20} seconds = 10^{-6} scaled units. Collisions that fell into this category were generally those involving molecules with high rotational energies. Very little computing time is used to recognize these cases since the step-size changing routine rapidly reaches this minimum step size for these collisions.

It is shown in the following section that it is convenient to give the initial rotational conditions of a molecule in terms of the angles θ and ϕ rather than the Cartesian coordinates $\vec{x}$ (suppressing the index j). These quantities are related by the expression $\vec{x} = (\sin\theta\cos\phi,\ \sin\theta\sin\phi,\ \cos\theta)$. The time derivatives are then obtained by differentiation

$$\dot{\vec{x}} = (\dot{\theta}\cos\theta\cos\phi - \dot{\phi}\sin\theta\sin\phi,\ \dot{\theta}\cos\theta\sin\phi + \dot{\phi}\sin\theta\cos\phi,\ -\dot{\theta}\sin\theta)$$

SELECTION OF INITIAL CONDITIONS

Since the scattering problem is a two-body calculation, it can be reduced to a problem involving only the rotational motion of the two molecules and their relative translational motion. The pertinent equations are described in the previous section. A complete set of initial conditions for these equations requires the selection of a "sample" molecule and a specification of its initial rotational motion, a specification of the initial rotational motion of a "heat bath" molecule, and a specification of their relative translational motion. All these assignments of initial conditions must be made in a manner that is consistent with the fact that (1) "heat bath" molecules are in an equilibrium distribution at a temperature T, (2) the "sample" and "heat bath" molecules are in translational equilibrium, and (3) the "sample" molecule has a known rotational energy.

First, the problem of the specification of the initial rotational state of a rigid-rod molecule is examined. If the effect of interactions is neglected, the rotational coordinates θ and ϕ and their conjugate momenta (see eq. (19))

$$\left.\begin{aligned} \frac{\partial T_{rot}}{\partial \dot{\theta}} &= p_\theta = I\dot{\theta} \\ \frac{\partial T_{rot}}{\partial \dot{\phi}} &= p_\phi = I\dot{\phi}\sin^2\theta \end{aligned}\right\} \tag{33}$$

have the normalized distribution

$$f_{rot}(\theta, \phi, p_\theta, p_\phi)d\theta\, d\phi\, dp_\theta\, dp_\phi = \frac{\beta}{8I\pi^2}\exp\left[-\frac{\beta}{2I}\left(\frac{p_\phi^2}{\sin^2\theta} + p_\theta^2\right)\right]d\theta\, d\phi\, dp_\theta\, dp_\phi \tag{34}$$

where $0 \le \theta \le \pi$, $0 \le \phi \le 2\pi$, $-\infty \le p_\theta \le \infty$, $-\infty \le p_\phi \le \infty$. If we introduce the transformation

$$\left.\begin{aligned} p_\phi &= \sqrt{I}\, p \sin\theta \cos\psi \\ p_\theta &= \sqrt{I}\, p \sin\psi \\ \theta &= \theta \\ \phi &= \phi \end{aligned}\right\} \tag{35}$$

with Jacobian $Ip \sin\theta$, the distribution takes the simpler factorized form

$$f_{rot}(p, \psi, \theta, \phi)\, dp\, d\psi\, d\theta\, d\phi = \exp\left[-\frac{\beta p^2}{2}\right] d\left(\frac{\beta p^2}{2}\right) \frac{d\psi}{2\pi} \frac{\sin\theta\, d\theta}{2} \frac{d\phi}{2\pi} \tag{36}$$

for $0 \leq p \leq \infty$, $0 \leq \psi \leq 2\pi$, $0 \leq \theta \leq \pi$, and $0 \leq \phi \leq 2\pi$. The new variable p effectively specifies the rotational energy, while ψ relates the two momenta p_θ and p_ϕ. Thus, from the first two members of equation (35), we readily deduce

$$T_{rot} = \frac{p^2}{2}$$

$$\psi = \tan^{-1}\left(\frac{p_\theta \sin\theta}{p_\phi}\right)$$

Each factor on the right is now a normalized one-variable distribution function for which the cumulative distribution (ref. 15, p. 23) can readily be obtained by integration. Therefore, we can pick at random from this distribution by using the method described by Schreider (ref. 21). In this method the cumulative distribution is equated to a random number R (numbers which are uniformly distributed over the interval $[0, 1]$), and the equation is then solved for the independent variable. This leads to

$$\left.\begin{aligned} p^2 &= -\left(\frac{2}{\beta}\right) \ln R_p \\ \psi &= 2\pi R_\psi \\ \theta &= \cos^{-1}(1 - 2R_\theta) \\ \phi &= 2\pi R_\phi \end{aligned}\right\} \tag{37}$$

where in the first of these equations we used the fact that if R is a random number, so too is $1 - R$. The subscripts on the various R's serve only to distinguish different random numbers. By combining equation (33) with equations (35) and (37), expressions are obtained for the quantities $\dot{\theta}$ and $\dot{\phi}$ which are used directly rather than p_θ and p_ϕ.

$$\left.\begin{aligned} \dot{\theta} &= \left[-\left(\frac{2}{\beta I}\right)\ln R_r\right]^{1/2} \sin 2\pi R_\psi \\ \dot{\phi} &= \frac{1}{2}\left[\frac{-2\ln R_p}{\beta I R_\theta(1-R_\theta)}\right]^{1/2} \cos 2\pi R_\psi \end{aligned}\right\} \tag{38}$$

Equation (38) and the last two members of equation (37) can be used to assign the rotational state of a randomly selected "heat bath" molecule. The orientation of a "sample" molecule may still be calculated from the last two members of equation (37); however, equation (38) cannot be used for their velocities since the rotational energy ϵ_i of the i^{th} "sample" molecule is known. Nevertheless, since p^2 is just twice the rotational energy, we may replace equation (38) with

$$\left.\begin{aligned} \dot{\theta}_i &= \left(\frac{2\epsilon_i}{I}\right)^{1/2} \sin 2\pi R_\psi \\ \dot{\phi}_i &= \frac{1}{2}\left[\frac{2\epsilon_i}{IR_\theta(1-R_\theta)}\right]^{1/2} \cos 2\pi R_\psi \end{aligned}\right\} \tag{39}$$

for the "sample" molecules.

There still remains the task of assigning the initial coordinates and momenta for the relative translational motion. The "sample" molecule is taken as the origin of the Cartesian, orthogonal coordinate system describing the relative motion (see fig. 3), while the "heat bath" molecule is situated on the negative Z-axis at a distance ρ from the origin. The initial separation distance was chosen as $\rho = 10$ Å. Let p_1, p_2, and p_3 be the translational momenta conjugate to X, Y, and Z, respectively. Obviously, if any scattering is to take place, p_3 must be greater than zero. Thus, it is appropriate to pick the p_i from the normalized flux distribution

$$f_{trans}(p_1,p_2,p_3)dp_1\,dp_2\,dp_3 = \left(\frac{\beta^2}{2\pi m^2}\right)\exp\left[\frac{-\beta\left(p_1^2+p_2^2+p_3^2\right)}{2m}\right]p_3\,dp_1\,dp_2\,dp_3 \tag{40}$$

for $0 \le p_3 \le \infty$, $-\infty \le p_1 \le \infty$, and $-\infty \le p_2 \le \infty$. If the transformation

$$\left.\begin{aligned} p_1 &= \left(\frac{2m}{\beta}\right)^{1/2} q \cos\varphi \\ p_2 &= \left(\frac{2m}{\beta}\right)^{1/2} q \sin\varphi \\ p_3 &= \left(\frac{2m}{\beta}\right)^{1/2} \bar{p} \end{aligned}\right\} \tag{41}$$

with Jacobian $(2m/\beta)^{3/2} q$ is introduced, f_{trans} becomes

$$f_{trans}(q, p, \varphi)dq\, d\bar{p}\, d\varphi = e^{-q^2} d(q^2)\, e^{-\bar{p}^2} d(\bar{p}^2) \frac{d\varphi}{2\pi} \tag{42}$$

for $0 \le q \le \infty$, $0 \le \bar{p} \le \infty$, and $0 \le \varphi \le 2\pi$. The variable q is just that part of the dimensionless relative kinetic energy that arises from the velocity components in the X-Y plane. The variable $\bar{p}$ is that part of the dimensionless relative kinetic energy that comes from the Z-component of velocity

$$q^2 = \frac{\beta^2\left(p_1^2 + p_2^2\right)}{2m}$$

$$\bar{p}^2 = \beta T_{trans} - q^2$$

Once again, the cumulative distribution function method can be used for picking from f_{trans}. This gives

$$\left.\begin{aligned} q &= (-\ln R_q)^{1/2} \\ \bar{p} &= (-\ln R_{\bar{p}})^{1/2} \\ \varphi &= 2\pi R_\varphi \end{aligned}\right\} \tag{43}$$

where in the first two equations we again used the fact that if R is a random number, then so too is $1 - R$. Combining equations (43) and (41) gives

$$\left.\begin{aligned} p_1 &= \left[-\left(\frac{2m}{\beta}\right)\ln R_q\right]^{1/2}\cos 2\pi R_\varphi \\ p_2 &= \left[-\left(\frac{2m}{\beta}\right)\ln R_q\right]^{1/2}\sin 2\pi R_\varphi \\ p_3 &= \left[-\left(\frac{2m}{\beta}\right)\ln R_{\overline{p}}\right]^{1/2} \end{aligned}\right\} \tag{44}$$

This completes the specification of the initial conditions for the scattering problem apart from the selection of the particular "sample" molecule that is to participate in the scattering. If the i^{th} molecule is to participate in the scattering, the index i is chosen by the prescription

$$i = \begin{cases} 1 + [NR_N] & R_N < 1 \\ N & R_N = 1 \end{cases} \tag{45}$$

where [a] represents the largest integer less than a.

DESCRIPTION OF COLLISON TRAJECTORIES

Time-history plots of relative translational velocity and target rotational energy and collision trajectories are shown in figures 4 and 5 for two types of collisions. The plots in figure 4 correspond to a reflecting collision, that is, a collision for which the distance of closest approach is σ. The plots in figure 5 correspond to a simple deflection collision, that is, a collision for which the distance of closest approach is greater than σ. All these plots were constructed by connecting N + 1 points, corresponding to N integration steps, by N straight lines. The plotting was terminated after no more than 250 integration steps.

A typical variation of the absolute value of the relative velocity is shown in figure 4(a) for a reflecting collision with an initial value of $|\dot{\vec{R}}|$ nearly thermal at T = 300 K. The corresponding variation in rotational energy of the target molecule is shown versus intermolecular separation in figure 4(b). The periodic character of both plots is due to the change in orientation angle between the dipoles. This oscillatory behavior becomes more irregular and of higher amplitude at small separations, where the dipole-dipole

interaction becomes strongest. Since the relative translational energy $mv^2/2 = 0.016$ eV is much greater than the rotational target energy $\epsilon \approx kT_0 = 0.002$ eV for these conditions ($T_{trans} = 300$ K; $T_{rot} = 25$ K), the change in $|\vec{R}|$ (~50 percent) is much smaller than the change in ϵ (a factor of 8). The projections of the incident heat bath molecule in the three Cartesian planes are shown in figures 4(c) to (e) for the simple reflection collision where the radial velocity changes sign at 3.36 Å. Similar plots are shown for a simple deflection collision in figures 5(a) to (c). The variation in initial velocity is relatively small since the turning point for relative motion is at 4.6 Å. The target rotor is still considerably perturbed since it is initially relatively "cold"; the rotational energy varies by about a factor of 5. The projection of the incident molecule's trajectory in the Y-Z plane is nearly a straight line. The projection of the motion onto the other two coordinate planes also gave straight lines.

RESULTS

Calculations have been performed for both HCl and DCl at two temperatures, 300 and 500 K. These four calculations were supplemented by 300 K calculations for two pseudo-HCl molecules which had the same molecular properties as HCl except for the dipole moment. In one case, the dipole moment was one-half the dipole moment of HCl; while in the other case, the dipole moment was 9/10 the value for HCl. These two pseudo-HCl molecules are designated HCl(1/2) and HCl(9/10). The molecular properties for the four molecules are listed in table I. Each of the six calculations was carried out for 3000 collisions on a sample of 50 molecules drawn at random from an equilibrium distribution of rotational energy at $T_0 = 25$ K. The same initial distribution was used in all six cases and corresponded to a mean initial rotational energy of $\beta_0 E_0 = 0.9464$.

Equation (4) was fitted to the results of the calculations both as a two parameter equation and a one parameter equation by the methods described in the appendix B. The two parameter fit was always superior to the one parameter fit, just as would be expected. The fitting was carried out after every 50 collisions, and the results are presented in figures 6 to 11. It is apparent that the choice $n_1 = 2000$ will satisfy the condition $n_1 > NZ_{rot}$ for all cases except for HCl(1/2) in the one parameter fitting of figure 11. In spite of this, $n_1 = 2000$ is used even in this case. Table II presents the mean values of the fitting constants in the interval [2000, 3000], as well as the initial relative kinetic energy E_{trans} and the initial rotational energy of the heat bath molecules E_{rot}, averaged over the 3000 collisions. Five of the six values of βE_∞ given in table II lie within 20 percent of unity, which agrees astonishingly well with the prediction of 84 percent given in figure 2. Similarly, the values of βE_{trans} are all within 5 percent of the

infinite population average of 2. The fact that βE_{trans} is consistently greater than the infinite population average of 2 is most likely a reflection of bias introduced by the process of rejecting initial conditions. The most obvious culprit of the three rejection categories is the rejection based on excessively long projected running times. This consistently rejects only collisions with low relative kinetic energies. This category represented 20 to 30 rejects for every 3000 collisions used. It is unlikely that any bias was introduced by the large-impact-parameter rejection category since this criterion only expresses a relation between the component of $\dot{\vec{R}}$ along the Z-axis and the other two components. Since the components are assigned randomly, this should reject some low relative kinetic energy collisions as well as some high energy collisions. However, initial conditions rejected because the step size was too small undoubtedly played a part. This was particularly obvious when we attempted to do calculations for HF. We found that, because of the strong dipole-dipole interaction, approximately 20 to 25 percent of the collisions that we attempted to calculate were being rejected because the step size became too small. This produced such a strong bias in βE_{trans} that we considered the calculations unusable. Typically, there were 800 to 1000 large-impact-parameter rejects, 20 to 30 long-integration-time rejects, and 20 to 30 step-size-too-small rejects for the calculations reported here.

Figures 12 to 14 display two exponential curves calculated from equation (4), as well as their asymptotic values and the data points for E_R after every 10 collisions. One curve was obtained using $\beta E_\infty = 1$ and the mean one parameter Z_{rot} for the interval [2000, 3000]. The other curve corresponds to the mean two parameter Z_{rot} for the interval 2000 to 3000 and the βE_∞ which minimizes the function Φ of appendix B for this Z_{rot}. Table III tabulates the function Φ for each pair of curves and also the value of Φ obtained by a direct one or two parameter least squares fitting of the 3000 data points. The data in table III clearly demonstrate the superiority of a two parameter fit over a one parameter fit since the value of Φ is always smaller for a two parameter fit. They also show that the mean Z_{rot} curves are only moderately inferior to the free Z_{rot} curves. A cursory examination of figures 12 to 14 discloses that an exponential does indeed seem to describe the evolution of the sample rotational energy but that the data scatter considerably about the fitted curve.

Table IV contains a summary of the experimental and theoretical Z_{rot} for HCl and DCl. The experimental numbers come from both thermal conductivity measurements and acoustic measurements. Even though the validity of the thermal conductivity numbers was questioned in reference 2, we nevertheless include them for comparison purposes. The acoustic numbers are the recent results obtained by Evans (ref. 22). He analyzed his measurements in terms of both a single and a double relaxation process and, further, he used a frequency dependent specific heat when calculating the classical absorption. The theoretical Z_{rot} were obtained from tabulations in reference 2, as well as from the calculations of this report. In the molecular dynamics results we have included not only

the mean Z_{rot} for the interval [2000, 3000], but also the extreme values in this interval. The latter are a more meaningful measure of the uncertainty in this case than the standard deviation.

Several qualitative observations can be made on the basis of the data in table IV. First, all the molecular dynamics results fall between the experimental data and the results of the perturbation calculation and, hence, are in closer agreement with experimental results. Second, all the numbers in table IV show that Z_{rot} increases with temperature except for those extracted from thermal conductivity measurements and the one parameter results for DCl. This is also apparent from table V. Third, all the theoretical numbers, except the one parameter, 300 K molecular dynamics data, show that increasing the moment of inertia decreases Z_{rot}. On the basis of these facts it seems that the two parameter data should be preferred over the one parameter results. Fourth, a comparison of HCl and HCl(1/2) shows that the dipole moment dependence of the molecular dynamics results is considerably weaker than the μ^4 dependence obtained in references 1 and 2; this is particularly true of the two parameter numbers.

We have shown that the results from the two parameter fit of the molecular dynamics calculations are in reasonable consonance with other theoretical predictions and, in addition, seem to be a closer approximation to the acoustic data than were the perturbation calculations of references 1 and 2. But this alone is insufficient evidence to inspire an overwhelming confidence in the results. Any such confidence is quickly tempered by the incongruous result for HCl(9/10) in table IV. Based on the values for HCl and HCl(1/2) we would expect Z_{rot} for HCl(9/10) to be quite close to that for HCl but still slightly larger. It is in fact considerably smaller. This opens two possibilities for consideration. The first is that 3000 collisions are insufficient to obtain an accurate Z_{rot}; the second possibility is that a 50-molecule sample is too small to give a precise value for Z_{rot}. The first option can be easily investigated by determining how close the fitted curves for E_R, shown in figures 12 and 14, are to their asymptotic values after 3000 collisions. This is shown in table VI. Obviously, in all cases 3000 collisions brings the sample within 91 percent of the asymptotic value for E_R except for the one parameter data for HCl(1/2). As a matter of fact, HCl and HCl(9/10) at 300 K are each within 5 percent of their asymptotic value. This certainly must eliminate the first possibility and leave us only with the second one. So it appears that even under the best of circumstances we must be prepared to accept an uncertainty in Z_{rot} of the order of six units, representing the difference between HCl and HCl(9/10) when working with such a small sample.

Finally, there is one additional aspect of the problem of determining Z_{rot} by molecular dynamics. To carry out the scattering calculations we were required to select an initial separation ρ. Our choice of an initial separation of $\rho = 10$ Å was dictated by pragmatic considerations. However, this choice committed us to the proposition that any potential collision with an impact parameter $b > \rho$ is not a physically significant

collision insofar as gas phase properties are concerned. Thus, in effect, we made a decision on what should be called a collision. However, in our computations we did more than this, since we rejected all collisions with impact parameters that exceeded $b_m = 2.5\,\sigma = 8.42$ Å. Thus, collisions whose impact parameters were in the range $8.42\text{ Å} < b \leq 10\text{ Å}$ were not counted. Although we cannot estimate the effect of our choice for ρ, we can quite easily place an upper limit on the effect of our choice for b_m. To do this we must know what fraction s of all physically significant collisions ($b \leq \rho$) have impact parameters less than, or equal to, b_m. But this is nothing more than the cumulative distribution function for b evaluated at b_m.

The impact parameter is related to the variables q and $\bar{p}$ of the translational distribution function (42) by

$$\left(\frac{b}{\rho}\right)^2 = \frac{q^2}{q^2 + \bar{p}^2}$$

Thus, in the space spanned by q^2, $\bar{p}^2$, the curves of constant impact parameter are the straight lines

$$\bar{p}^2 = q^2\left[\frac{1 - \left(\frac{b^2}{\rho^2}\right)}{\frac{b^2}{\rho^2}}\right]$$

Thus, the cumulative distribution function for b is given by the integral

$$\int_0^{\infty} d(\bar{p}^2) \int_0^{(b^2/\rho^2)\bar{p}^2/(1-b^2/\rho^2)} d(q^2)\, \exp\left[-(\bar{p}^2 + q^2\right] = \frac{b^2}{\rho^2}$$

Therefore, it follows that $s = b_m^2/\rho^2$. If we now reasonably assume that collisions with $b > b_m$ are uniformly distributed during the course of the calculation, the choice of $b_m < \rho$ implies a uniform scale change in the abscissa n, $n = n's$. Hence, since $n/NZ_{rot} = n'/NZ'_{rot}$, we conclude that $Z'_{rot} = Z_{rot}/s = \rho^2 Z_{rot}/b_m^2$. Incorporating our choice of ρ and b_m results in $Z'_{rot} = 1.41\, Z_{rot}$. This is clearly an upper limit to the effect since this presumes that the ordinate E_R is unaffected. In spite of the fact that the neglected collisions would not be responsible for a large fraction of the total energy transferred to the sample molecules, they could transfer some energy. This is particularly true during the initial phases of the calculation, when the net effect should be to in-

crease the energy absorption by the cold sample molecules. This could somewhat compensate for the stretching of the abscissa. Interestingly enough, the effect we have been discussing serves to bring the rotational collision numbers somewhat closer to the values obtained by the perturbation calculation. This is shown in table VII which gives Z_{rot}, Z'_{rot}, and the numbers obtained by the perturbation calculation for HCl and DCl. Although, the values of Z'_{rot} are closer to the perturbation results, they are further away from the experiment acoustic values than Z_{rot}.

CONCLUSIONS

The discussions of the previous section can be summarized as follows:

1. The mean rotational energy of the sample molecules exhibits an exponential approach to a steady state value; however, there is considerable scatter about the exponential curve.

2. The molecular dynamics results for HCl and DCl are generally in consonance with previous perturbation calculations.

3. The values of Z_{rot} for HCl and DCl obtained by molecular dynamics are intermediate to the experimental Z_{rot} values and those obtained by a perturbation calculation.

Lewis Research Center,
National Aeronautics and Space Administration,
Cleveland, Ohio, February 10, 1971,
129-01.

APPENDIX A

STEP-SIZE CONTROL

The integration step size was determined by an empirical technique based on (1) the conservation of energy E during a collision, (2) a specified maximum allowable error in the energy, $\Delta E > 0$, and (3) an estimated total trajectory time T. If $E^{(0)} > 0$ is the initial energy, $h^{(i)}$ is the step size to be taken in the next integration step, $t^{(i+1)} = t^{(i)} + h^{(i)}$, and $E^{(i)}$ and $E^{(i+1)}$ are the values of the energy before and after the step, respectively, then the step produces an actual error increment in the energy that may be expressed as

$$\delta_a^{(i+1)} = \left| \frac{E^{(i+1)} - E^{(i)}}{E^{(0)}} \right| \tag{A1}$$

On the other hand, a maximum tolerated error increment for the step is defined by

$$\delta_t^{(i+1)} = \frac{\left[\Delta E - \left| E^{(i)} - E^{(0)} \right| \right] h^{(i)}}{E^{(0)} T} \tag{A2}$$

At the conclusion of each step we calculate

$$\Delta^{(i+1)} \equiv \frac{\delta_a^{(i+1)}}{\delta_t^{(i+1)}} = \frac{\left| E^{(i+1)} - E^{(i)} \right|}{\Delta E - \left| E^{(i)} - E^{(0)} \right|} \frac{T}{h^{(i)}} \tag{A3}$$

If $0 \leq \Delta^{(i+1)} \leq 2$, the step is accepted; otherwise, it is rejected. In either case, a new step size is chosen by the prescription

$$\frac{h^{(i+1)}}{h^{(i)}} = \min \left\{ 4, \left[\Delta^{(i+1)} \right]^{m+1} \right\} \tag{A4}$$

where m is the order of the Runge-Kutta integration routine.

This prescription for altering the step size can lead to either a larger or a smaller step size. Should the step size become smaller than 10^{-20} second, the calculation is terminated. Fortunately, such a situation rarely occurs.

APPENDIX B

LEAST SQUARES FITTING

There are three available parameters to fit equation (4) to the sample rotational energy data in a least squares sense, namely, E_0, E_∞, and Z_{rot}. We chose E_0 so that the curve would pass through the known rotational energy prior to any collisions. This leaves only E_∞ and Z_{rot}. The parameter E_∞ presumably corresponds to the equilibrium value which is equal to kT for an infinite population of molecules with two rotational degrees of freedom. But for a sample of only 50 molecules, based on our statistical considerations (fig. 2), there is no assurance that E_∞ will turn out to be kT. Thus we determined both E_∞ and Z_{rot} by the least squares fitting procedure.

At this point it becomes convenient to introduce some alternate notation. Thus, we define

$$\mathscr{E} = \beta(E_R - E_0) \tag{B1}$$

and introduce new parameters by

$$\left.\begin{aligned} A &= \beta(E_\infty - E_0) \\ x &= Z_{rot}^{-1} \end{aligned}\right\} \tag{B2}$$

Then equation (4) becomes the function

$$\mathscr{E}(n) = A\left[1 - \exp\left(-\frac{nx}{N}\right)\right] \tag{B3}$$

If we denote the tabulated data by $\overline{\mathscr{E}}(n)$, we can define

$$\Phi(x, A) = \frac{1}{2}\sum_{n=1}^{M}\left[\mathscr{E}(n) - \overline{\mathscr{E}}(n)\right]^2 \tag{B4}$$

where M is the total number of points used in the fitting. The expression for the sum of a geometric series can be used to reexpress Φ in the form

$$\Phi(x, A) = \frac{A^2}{2}\left[M + 1 - 2g(x) + g(2x)\right] - A\left[\sum_{n=1}^{M} \bar{\mathscr{E}}(n) - \sum_{n=1}^{M} \bar{\mathscr{E}}(n)e^{-nx/N}\right]$$

$$+ \frac{1}{2}\sum_{n=1}^{M} \bar{\mathscr{E}}^2(n) \qquad \text{(B5)}$$

where

$$g(x) = \frac{1 - \exp\left[-\dfrac{(M+1)x}{N}\right]}{1 - \exp\left[-\dfrac{x}{N}\right]} \qquad \text{(B6)}$$

The function $g(x)$ is monotonically decreasing and has the limiting values

$$\left.\begin{aligned} g(0) &= M + 1 \\ g(\infty) &= 1 \end{aligned}\right\} \qquad \text{(B7)}$$

Thus, it follows that Φ has the limiting values

$$\left.\begin{aligned} \Phi(0, A) &= \frac{1}{2}\sum_{n=1}^{M} \bar{\mathscr{E}}^2(n) \\ \Phi(\infty, A) &= \frac{1}{2}MA^2 - A\sum_{n=1}^{M} \bar{\mathscr{E}}(n) + \frac{1}{2}\sum_{n=1}^{M} \bar{\mathscr{E}}^2(n) \end{aligned}\right\} \qquad \text{(B8)}$$

The parameters A and x are determined so as to minimize Φ; that is, they are solutions of the equations

$$\left.\begin{aligned} \frac{\partial \Phi}{\partial A} &= A[M + 1 - 2g(x) + g(2x)] - \sum_{n=1}^{M} \bar{\mathcal{E}}(n)(1 - e^{-nx/N}) = 0 \\ NA^{-1} \frac{\partial \Phi}{\partial x} &= AN[g'(2x) - g'(x)] - \sum_{n=1}^{M} n\, \bar{\mathcal{E}}(n)\, e^{-nx/N} = 0 \end{aligned}\right\} \tag{B9}$$

where the primes are used to symbolize differentiation with respect to x. The first of these immediately gives A as a function of x.

$$A(x) = \frac{\sum_{n=1}^{M} \bar{\mathcal{E}}(n)(1 - e^{-nx/N})}{M + 1 - 2g(x) + g(2x)} \tag{B10}$$

We now define a function of x alone as

$$G(x) \equiv NA^{-1} \frac{\partial \Phi}{\partial x}\bigg|_{A=A(x)} \tag{B11}$$

The solution of the equation

$$G(x) = 0 \tag{B12}$$

can now be accomplished by the Newton-Raphson iteration (ref. 23)

$$\left.\begin{aligned} x^{(i+1)} &= x^{(i)} + \lambda\, \Delta x^{(i)} \\ \Delta x^{i} &= \frac{-\, G(x^{(i)})}{G'(x^{(i)})} \end{aligned}\right\} \tag{B13}$$

where $0 < \lambda \leq 1$ is a convergence control parameter. The iteration is carried out by using the following expressions:

$$G'(x) = A'N\left[g'(2x) - g'(x)\right] + AN\left[2g''(2x) - g''(x)\right] + \sum_{n=1}^{M} n^2 \bar{\mathscr{E}}(n) \frac{e^{-nx/N}}{N}$$

$$A'(x) = \frac{\sum_{n=1}^{M} n\,\bar{\mathscr{E}}(n) \frac{e^{-nx/N}}{N} + 2[g'(x) - g'(2x)]A}{M + 1 - 2g(x) + g(2x)}$$

$$Ng'(x) = \frac{M + 1 - g(x)}{1 - e^{-x/N}} - Mg(x)$$

$$Ng''(x) = -\frac{M + 1}{1 - e^{-x/N}} g'(x) - \frac{[M + 1 - g(x)]e^{-x/N}}{\left(1 - e^{-x/N}\right)^2 N}$$

The actual procedure used was to make an initial estimate for x, calculate $A(x)$ from equation (B10) and obtain a new estimate for x from equation (B13). The iteration was terminated whenever $|\Delta x^{(i)}| \leq 10^{-6}$.

When E_∞ was not to be treated as a fitting parameter, we set $A = 1 - (E_0/kT)$ and $A' = 0$ and proceeded as before. When Z_{rot} was not to be treated as a fitting parameter, A could be calculated directly from equation (B10).

REFERENCES

1. Zeleznik, Frank J.: Rotational Relaxation in Polar Gases. J. Chem. Phys., vol. 47, no. 9, Nov. 1, 1967, pp. 3410-3424.

2. Zeleznik, Frank J.; and Svehla, Roger A.: Rotational Relaxation in Polar Gases. II. J. Chem. Phys., vol. 53, no. 2, July 15, 1970, pp. 632-646.

3. Rahman, A.: Correlations in the Motion of Atoms in Liquid Argon. Phys. Rev., vol. 136A, no. 2, Oct. 19, 1964, pp. 405-411.

4. Rahman, Aneesur: Liquid Structure and Self-Diffusion. J. Chem. Phys., vol. 45, no. 7, Oct. 1, 1966, pp. 2585-2592.

5. Verlet, Loup: Computer "Experiments" on Classical Fluids. I. Thermodynamical Properties of Lennard-Jones Molecules. Phys. Rev., vol. 159, no. 1, July 5, 1967, pp. 98-103.

6. Verlet, Loup: Computer "Experiments" on Classical Fluids. II. Equilibrium Correlation Functions. Phys. Rev., vol. 165, no. 1, July 5, 1968, pp. 201-214.

7. Fehder, Paul L.: Molecular Dynamics Studies of the Microscopic Properties of Dense Fluids. J. Chem. Phys., vol. 50, no. 6, Mar. 15, 1969, pp. 2617-2629.

8. Köhler, M.; and Bellemans, A.: Molecular Dynamics of Weakly Coupled Electric Dipoles on a Rigid Lattice. I. The Approach to Equilibrium. J. Chem. Phys., vol. 47, no. 4, Aug. 15, 1967, pp. 1261-1265.

9. Bellemans, A.; Köhler, M.; and Gancberg, M.: Molecular Dynamics of Weakly Coupled Electric Dipoles on a Rigid Lattice. II. The Dielectric Response Function. J. Chem. Phys., vol. 51, no. 6, Sept. 15, 1969, pp. 2578-2586.

10. Hirooka, Hajime; and Saitô, Nobuhiko: Computer Studies on the Approach to Thermal Equilibrium in Coupled Anharmonic Oscillators. I. Two Dimensional Case. J. Phys. Soc. Japan, vol. 26, no. 3, Mar. 1969, pp. 624-630.

11. Alterman, Elliott B.; and Wilson, David J.: Vibrational Energy Transfer in Gases. Atom-Diatomic Molecule Collisions. J. Chem. Phys., vol. 42, no. 6, Mar. 15, 1965, pp. 1957-1961.

12. Raff, L. M.: Theoretical Investigations of Translation-Rotation Energy Transfer: (H_2, He) and D_2, He) Systems. J. Chem. Phys., vol. 46, no. 2, Jan. 15, 1967, pp. 520-531.

    Raff, L. M.: Erratum: Theoretical Investigations of Translation-Rotation Energy Transfer: (H_2, He) and (D_2, He) Systems. J. Chem. Phys., vol. 47, no. 5, Sept. 1, 1967, p. 1884.

13. Berend, George C.; and Benson, Sidney W.: Classical Theory of Rotational Relaxation of Diatomic Molecules. J. Chem. Phys., vol. 47, no. 10, Nov. 15, 1967, pp. 4199-4202.

14. Jonkman, M.; and Ertas, I.: Translational-Rotational Relation Times in Gaseous Mixtures. Molecular Relaxation Processes. Academic Press, Inc., 1966, p. 235.

15. Hoel, Paul G.: Introduction to Mathematical Statistics. Third ed., John Wiley & Sons, Inc., 1963.

16. Harter, H. Leon: New Tables of the Incomplete Gamma-Function Ratio of Percentage Points of the Chi-Square and Beta Distributions. U.S. Air Force, Office of Aerospace Research Labs., 1964.

17. Goldstein, Herbert: Classical Mechanics. Addison-Wesley Publ. Co., Inc., 1950, p. 107.

18. Dugan, John V., Jr.; and Magee, John L.: Capture Collisions Between Ions and Polar Molecules. J. Chem. Phys., vol. 47, no. 9, Nov. 1, 1967, pp. 3103-3112.

19. Pars, L. A.: An Introduction to the Calculus of Variations. John Wiley & Sons, Inc., 1962, p. 222.

20. Elsgolc, L. E.: Calculus of Variations. Pergamon Press, 1961, p. 127.

21. Shreider, Yu. A., ed.: The Monte Carlo Method. Pergamon Press, 1966, p. 314.

22. Evans, L. B.: Rotational Relaxation in Polar Gases. Ph. D. Thesis, Oklahoma State Univ., 1969.

23. Hildebrand, Francis B.: Introduction to Numerical Analysis. McGraw-Hill Book Co., Inc., 1956, p. 447.

24. Monchick, L.; and Mason, E. A.: Transport Properties of Polar Gases. J. Chem. Phys., vol. 35, no. 5, Nov. 1961, pp. 1676-1697.

TABLE I. - MOLECULAR PROPERTIES

[Molecular diameter[a], 3.36×10^{-8} cm (3.36×10^{-10} m).]

Molecule	Molecular weight	Moment of inertia, I, g-cm^2	Dipole moment, μ, esu-cm
HCl	36.461	2.6431×10^{-40}	1.081×10^{-18}
DCl	37.467	5.1404	1.085
HCl(1/2)	36.461	2.6431	.541
HCl(9/10)	36.461	2.6431	.973

[a]All molecular diameters set equal to that of HCl, which was obtained from an analysis of viscosity data made by using the Stockmayer potential (ref. 24).

TABLE II. - MEAN FITTING PARAMETERS IN INTERVAL 2000 TO 3000 AND MEAN RELATIVE KINETIC ENERGY AND HEAT BATH MOLECULE ROTATIONAL ENERGY FOR 3000 COLLISIONS

Molecule	Temperature, K	Two parameter fit		Rotational collision number Z_{rot} for one parameter fit	Mean relative kinetic energy, βE_{trans}	Heat bath molecule rotational energy for 3000 collisions, βE_{rot}
		Dimensionless rotational energy, βE_∞	Rotational collision number, Z_{rot}			
HCl	300	1.17	19.0	12.9	2.10	0.98
HCl	500	1.07	24.4	21.1	2.07	.98
DCl	300	.97	14.2	15.6	2.06	1.00
DCl	500	1.19	21.7	14.4	2.03	.99
HCl(1/2)	300	.64	22.3	51.7	2.04	.97
HCl(9/10)	300	1.02	12.9	12.2	2.08	1.00

TABLE III. - THE FUNCTION Φ AFTER 3000 COLLISIONS

Molecule	Temperature, K	Φ for two parameter fit, rotational collision number Z_{rot} -		Φ for one parameter fit, rotational collision number Z_{rot} -	
		Free	Fixed at mean	Free	Fixed at mean
HCl	300	10.462	10.478	18.095	18.138
HCl	500	2.883	2.902	3.667	3.703
DCl	300	7.083	7.357	8.727	8.774
DCl	500	4.458	4.910	17.374	17.537
HCl(1/2)	300	1.236	1.446	2.576	2.693
HCl(9/10)	300	10.983	12.256	14.747	14.803

TABLE IV. - EXPERIMENTAL AND THEORETICAL ROTATIONAL COLLISION NUMBERS Z_{rot} FOR HCl AND DCl

(a) Experimental

Molecule	Temperature, K	Rotational collision number Z_{rot} obtained from-		
		Thermal conductivity measurements[a]	Acoustic measurements[b]	
			Single-relaxation process	Double-relaxation process
HCl	300	3.8	6.4	3.0
HCl	500	1.0	[c]9.6	[c]4.3
DCl	300	.9	---	---
DCl	500	0	---	---
HCl(1/2)	300	---	---	---
HCl(9/10)	300	---	---	---

(b) Theoretical

Molecule	Temperature, K	Rotational collision number Z_{rot} calculated by-					
		Perturbation calculation[d]	Molecular dynamics[e]				
			Two parameter fit			One parameter fit	
			Mean	Max.	Min.	Mean	Max.	Min.
HCl	300	65.9	19.0	21.2	17.5	12.9	13.2	12.6
HCl	500	79.8	24.4	27.1	23.2	21.1	21.4	20.8
DCl	300	51.9	14.2	16.1	12.7	15.6	16.0	15.3
DCl	500	64.2	21.7	25.0	18.7	14.4	15.0	13.8
HCl(1/2)	300	----	22.3	27.4	19.1	51.7	53.4	48.7
HCl(9/10)	300	----	12.9	16.4	10.0	12.2	12.5	11.8

[a]Taken from table III of ref. 2.

[b]Data of L. B. Evans (ref. 22).

[c]Read from a curve faired through data of L. B. Evans (ref. 22).

[d]Taken from table IV of ref. 2.

[e]This work.

TABLE V. - TEMPERATURE DEPENDENCE OF ROTATIONAL COLLISION NUMBER Z_{rot} FOR HCl AND DCl

Source	$Z_{rot}(300\ K)/Z_{rot}(500\ K)$	
	HCl	DCl
Experimental:		
Thermal conductivity	3.8	∞
Acoustics		
Single-relaxation process	.67	----
Double-relaxation process	.70	----
Theoretical:		
Perturbation calculation	.83	0.81
Molecular dynamics		
Two parameter fit	.78	.66
One parameter fit	.61	1.08

TABLE VI. - APPROACH OF SAMPLE ROTATIONAL ENERGY E_R TO ITS ASYMPTOTIC VALUE AFTER 3000 COLLISIONS

Molecule	Temperature, K	$[E_R(3000) - E_0]\ (E_\infty - E_0)^a$	
		Two parameter fit	One parameter fit
HCl	300	0.9572	0.9903
HCl	500	.9142	.9415
DCl	300	.9855	.9787
DCl	500	.9372	.9845
HCl(1 2)	300	.9326	.6865
HCl(9 10)	300	.9904	.9927

[a]Calculated by eq. (4) using the data given in figs. 12 to 14.

TABLE VII. - COMPARISON OF THEORETICAL

ROTATIONAL COLLISION NUMBERS

Molecule	Temperature, K	Rotational collision number, determined by-				
		Perturbation calculation	Molecular dynamics			
			Two parameter fit		One parameter fit	
			Z_{rot}	Z'_{rot}	Z_{rot}	Z'_{rot}
HCl	300	65.9	19.0	26.8	12.9	18.2
HCl	500	79.8	24.4	34.4	21.1	29.8
DCl	300	51.9	14.2	20.0	15.6	22.0
DCl	500	64.2	21.7	30.6	14.4	20.3

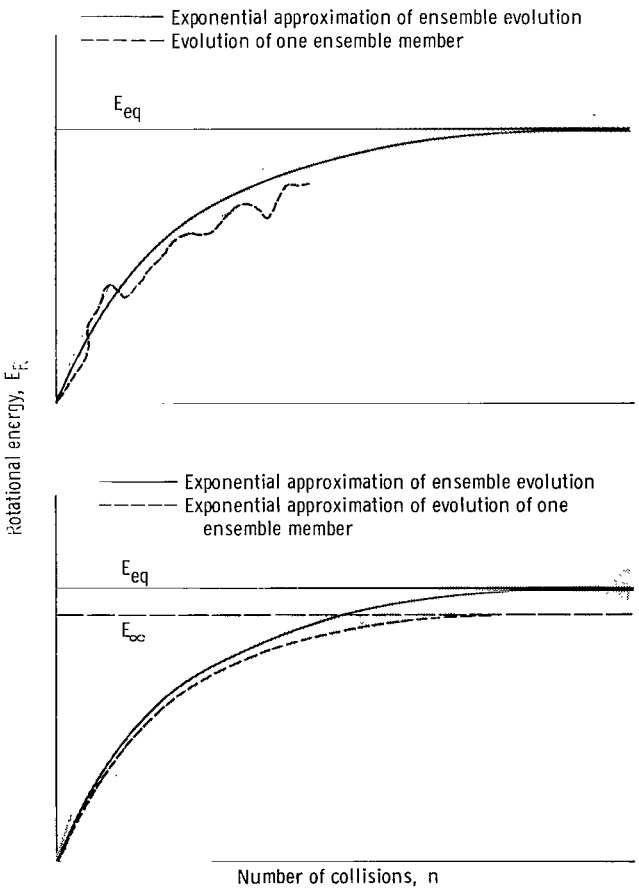

Figure 1. - Temporal evolution of rotational energy of ensemble. Shading represents density of data points.

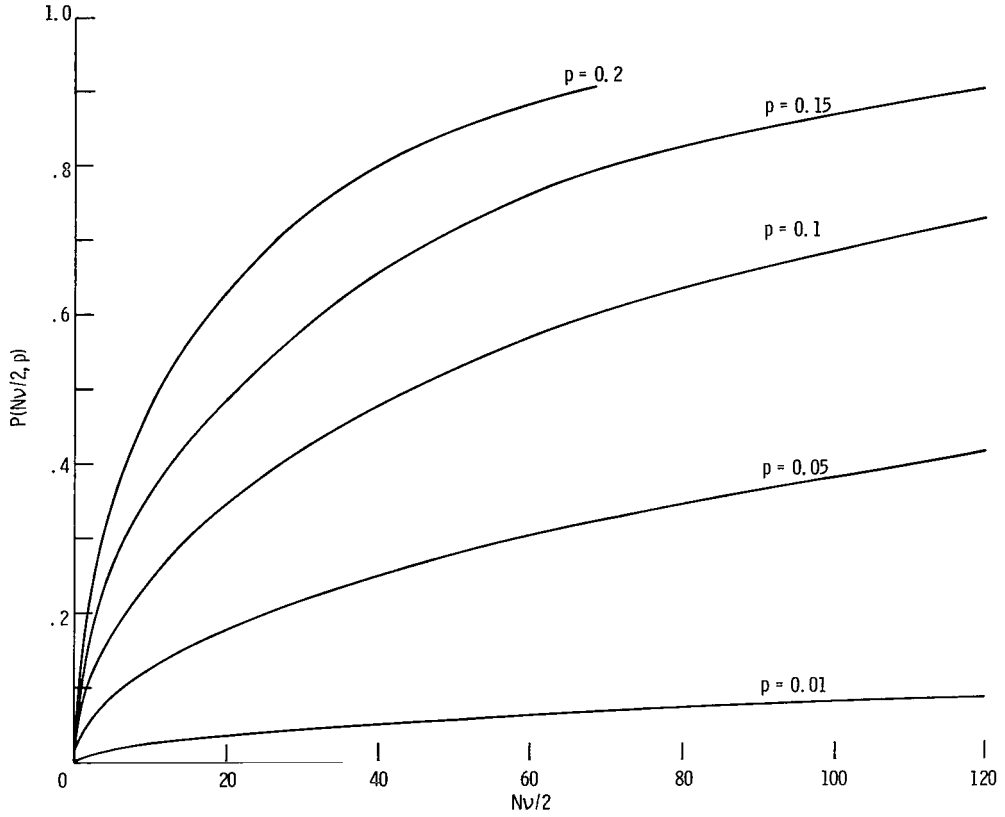

Figure 2. - Probability that a random sample of size N drawn from a χ^2 distribution with ν degrees of freedom lies in the interval $(1 \pm p)\mu_1$, about the mean μ_1.

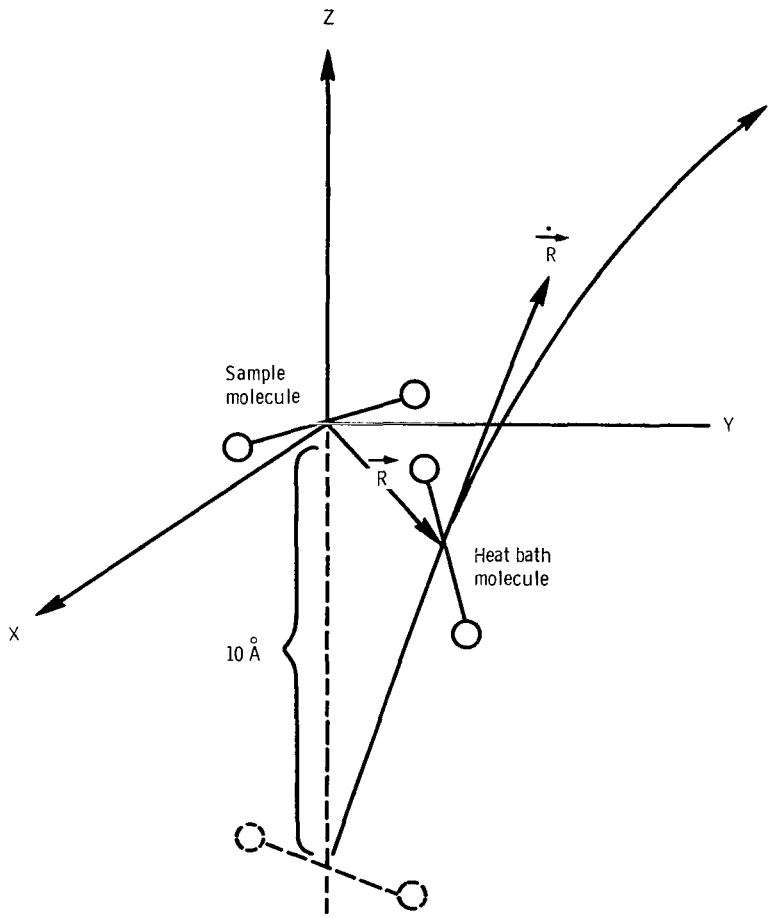

Figure 3. - Relative motion of molecules.

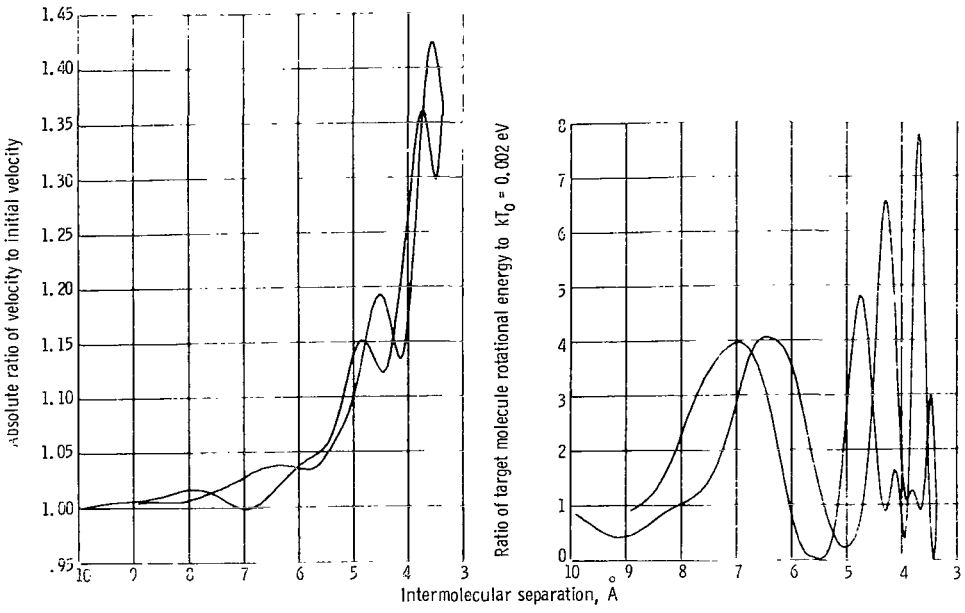

(a) Relative translational velocity. Initial velocity, 4.1×10^4 centimeters per second.

(b) Target rotational energy.

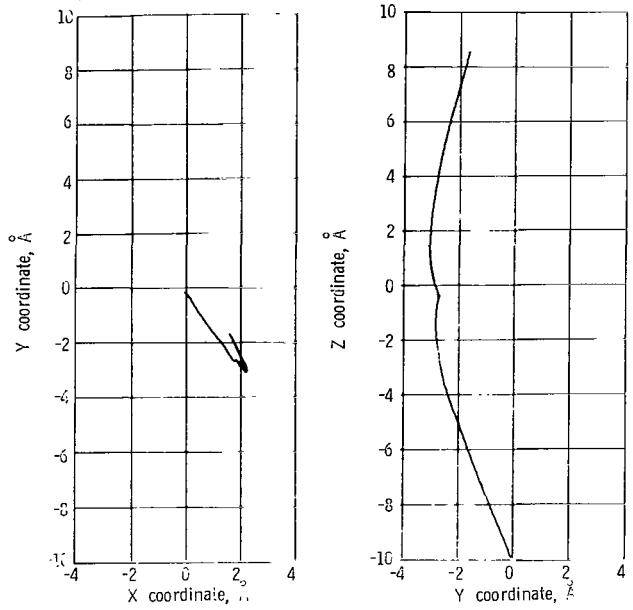

(c) Collision trajectory in X-Y plane.

(d) Collision trajectory in Y-Z plane.

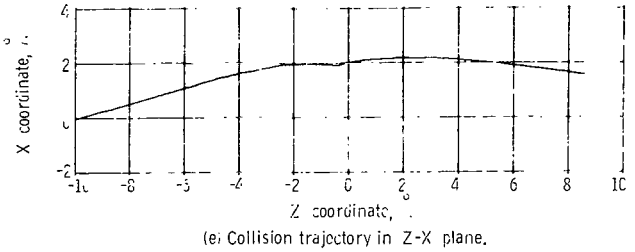

(e) Collision trajectory in Z-X plane.

Figure 4. - Time-history plots of relative translational velocity, target rotational energy, and collision trajectories for a reflection collision.

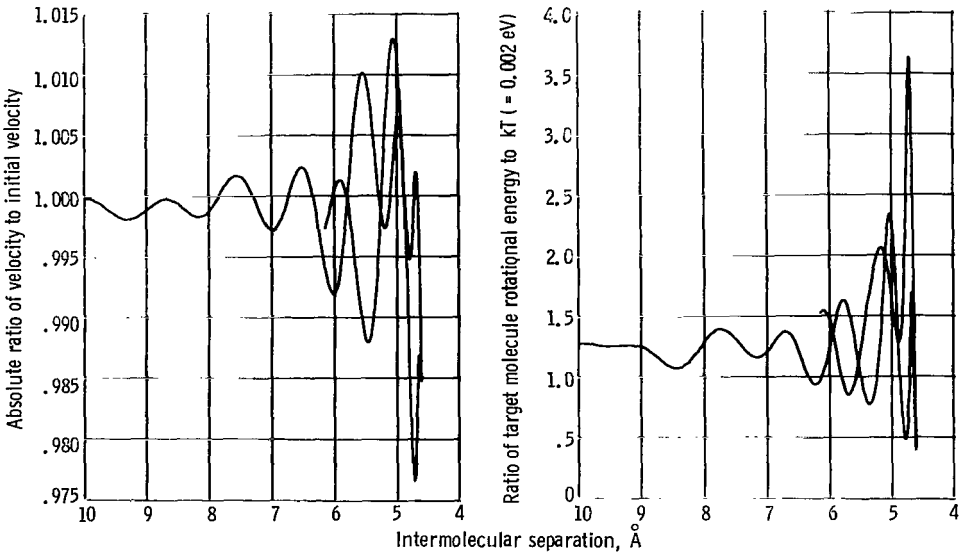

(a) Relative translational velocity. Initial velocity, 5.95×10^4 centimeters per second.

(b) Target rotational energy.

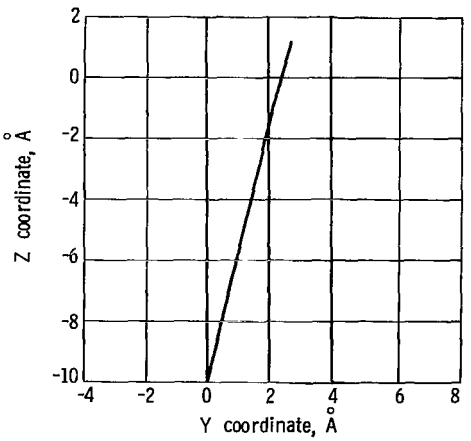

(c) Collision trajectory in Y-Z plane.

Figure 5. - Time-history plots of relative translational velocity, target rotational energy, and collision trajectory for a simple deflection collision.

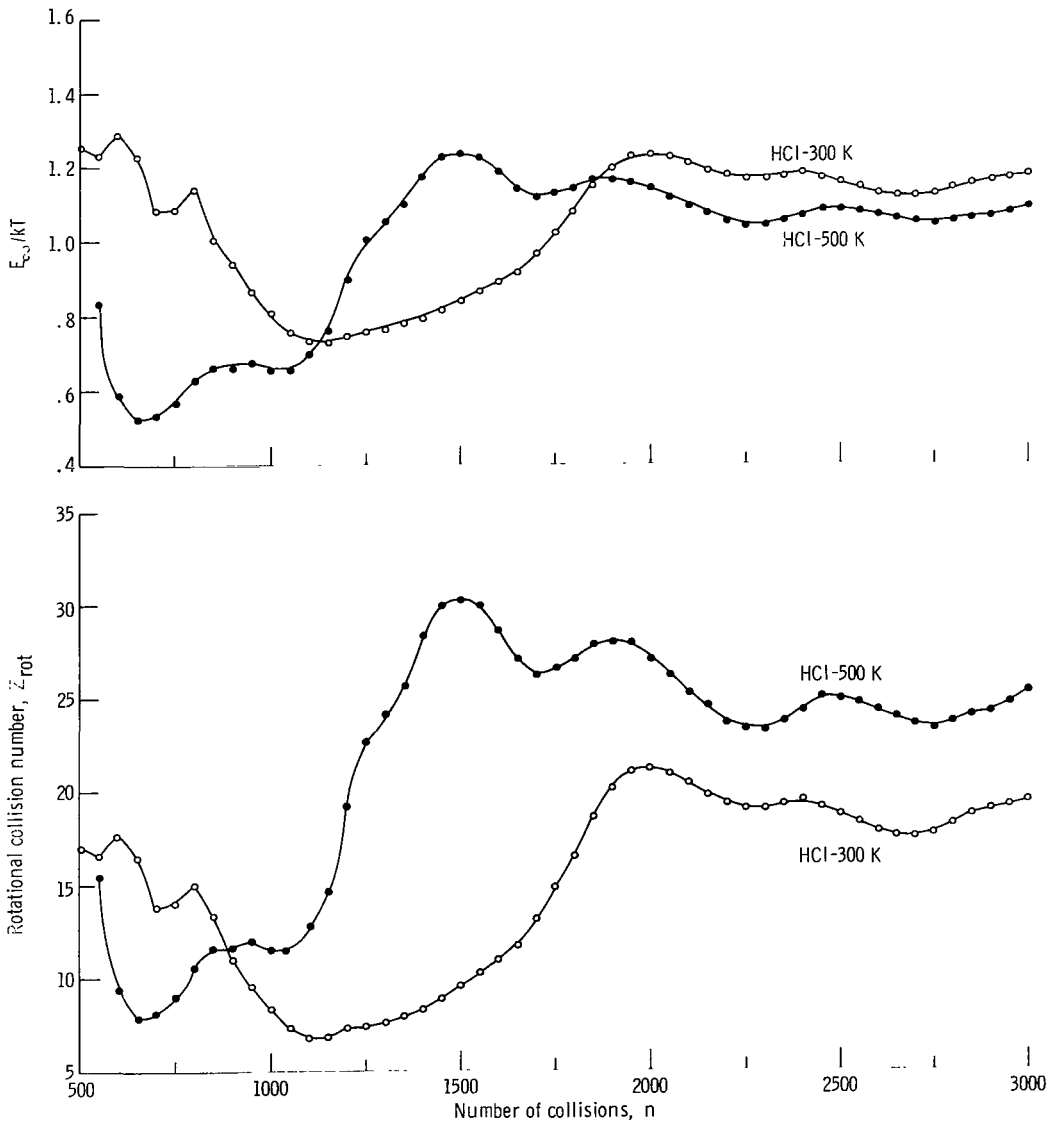

Figure 6. - Least squares fitting constants for HCl as function of the number of collisions: two parameter analysis.

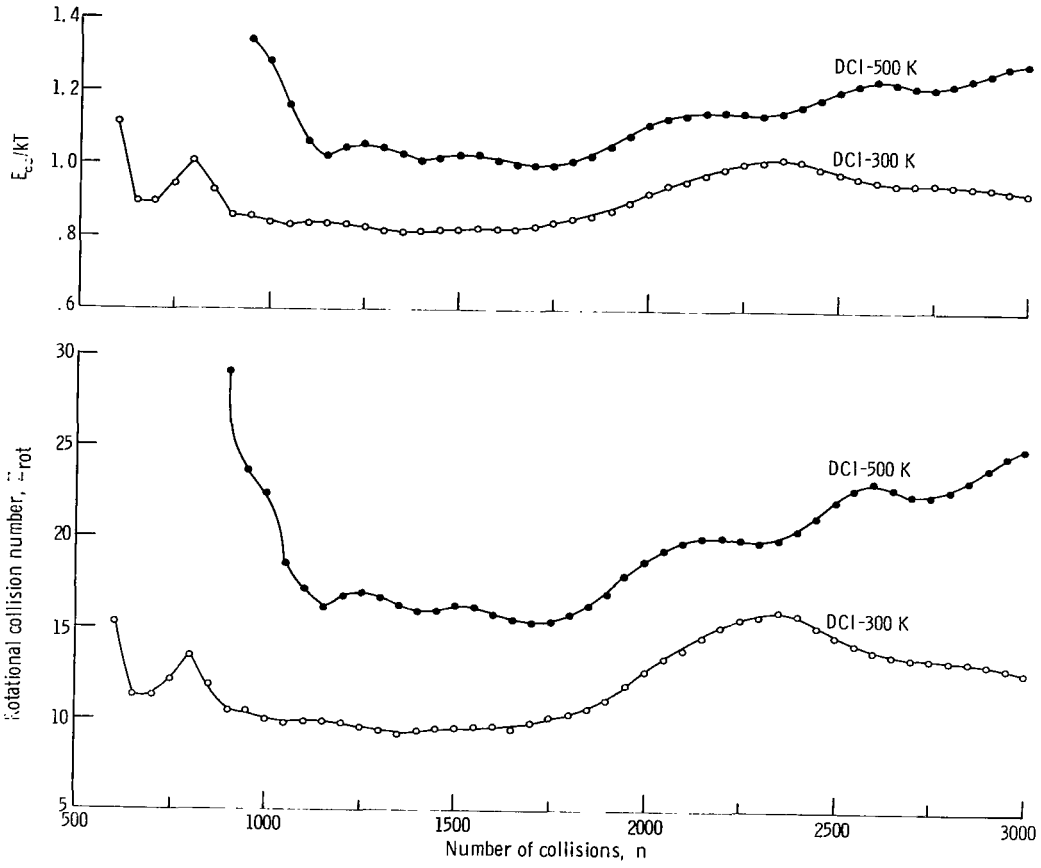

Figure 7. - Least squares fitting constants for DCl as a function of the number of collisions: two parameter analysis.

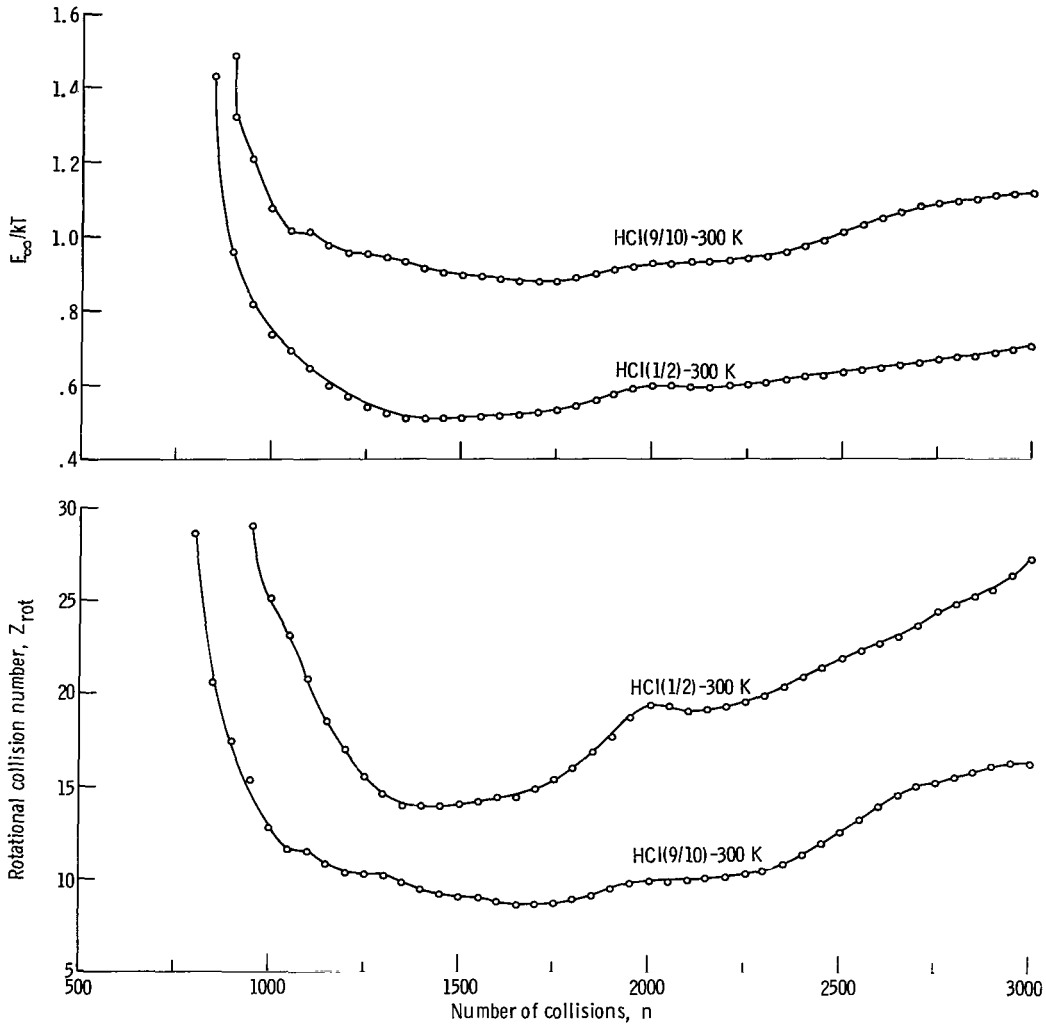

Figure 8. - Least squares fitting constants for HCl(1/2) and HCl(9/10) as a function of the number of collisions: two parameter analysis; temperature, 300 K.

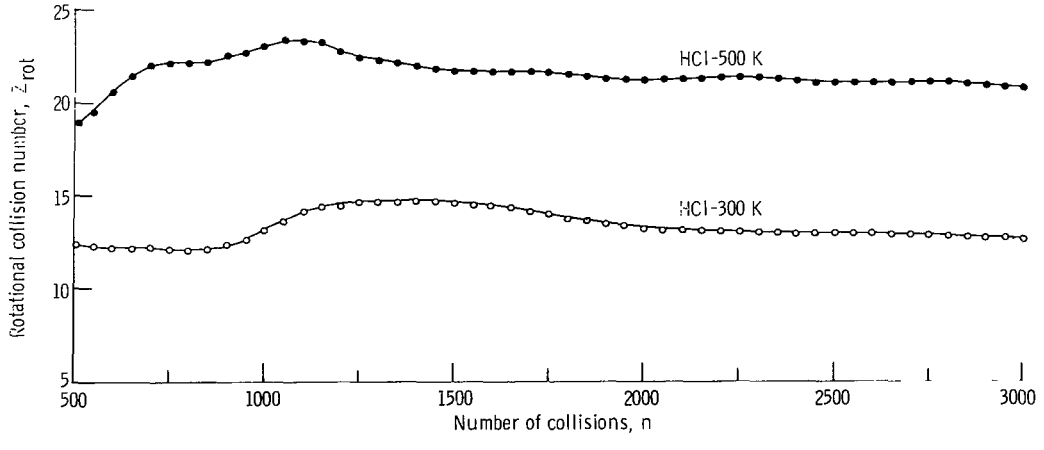

Figure 9. - Least squares fitting constant for HCl as a function of the number of collisions: one parameter analysis.

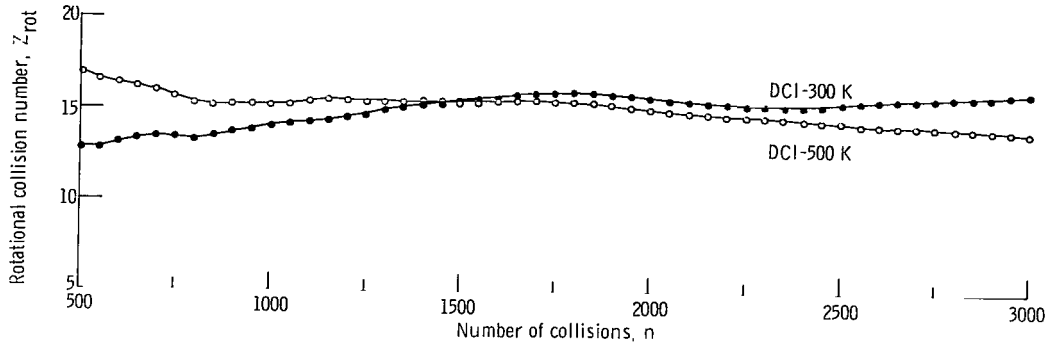

Figure 10. - Least squares fitting constant for DCl as a function of the number of collisions: one parameter analysis.

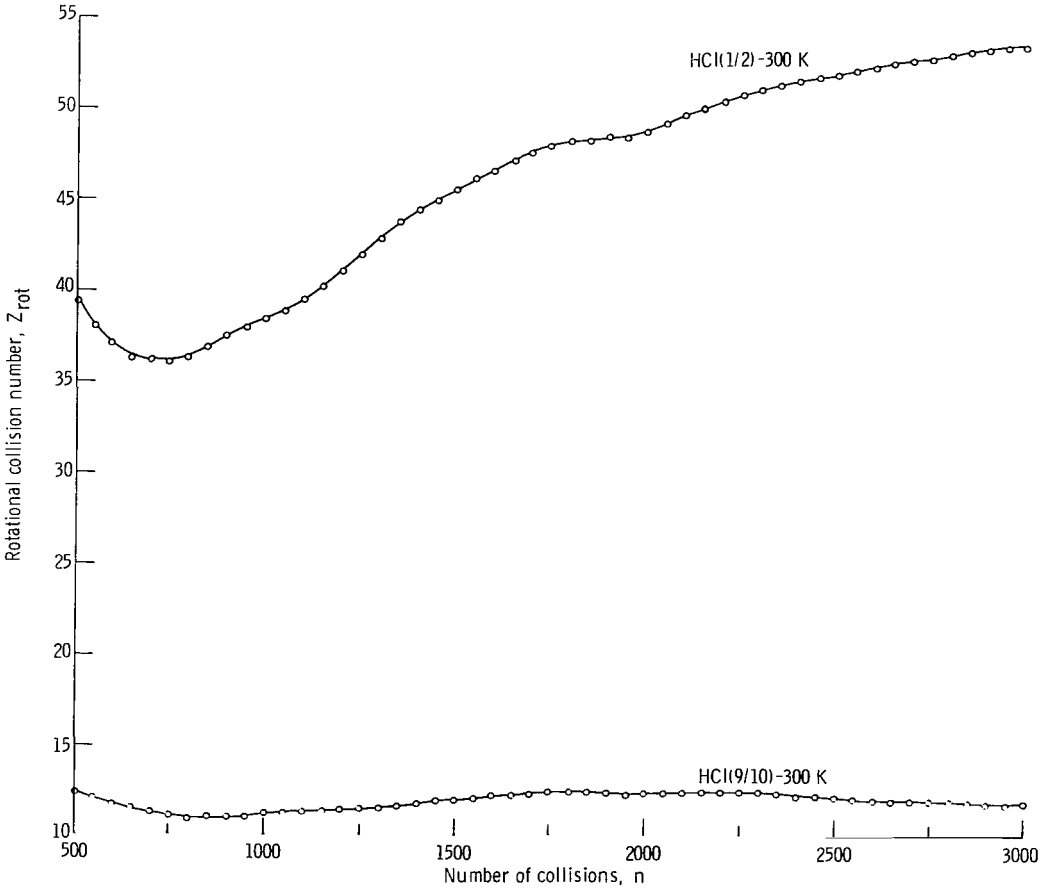

Figure 11. - Least squares fitting constant for HCl(1/2) and HCl(9/10) as a function of the number of collisions: one parameter analysis.

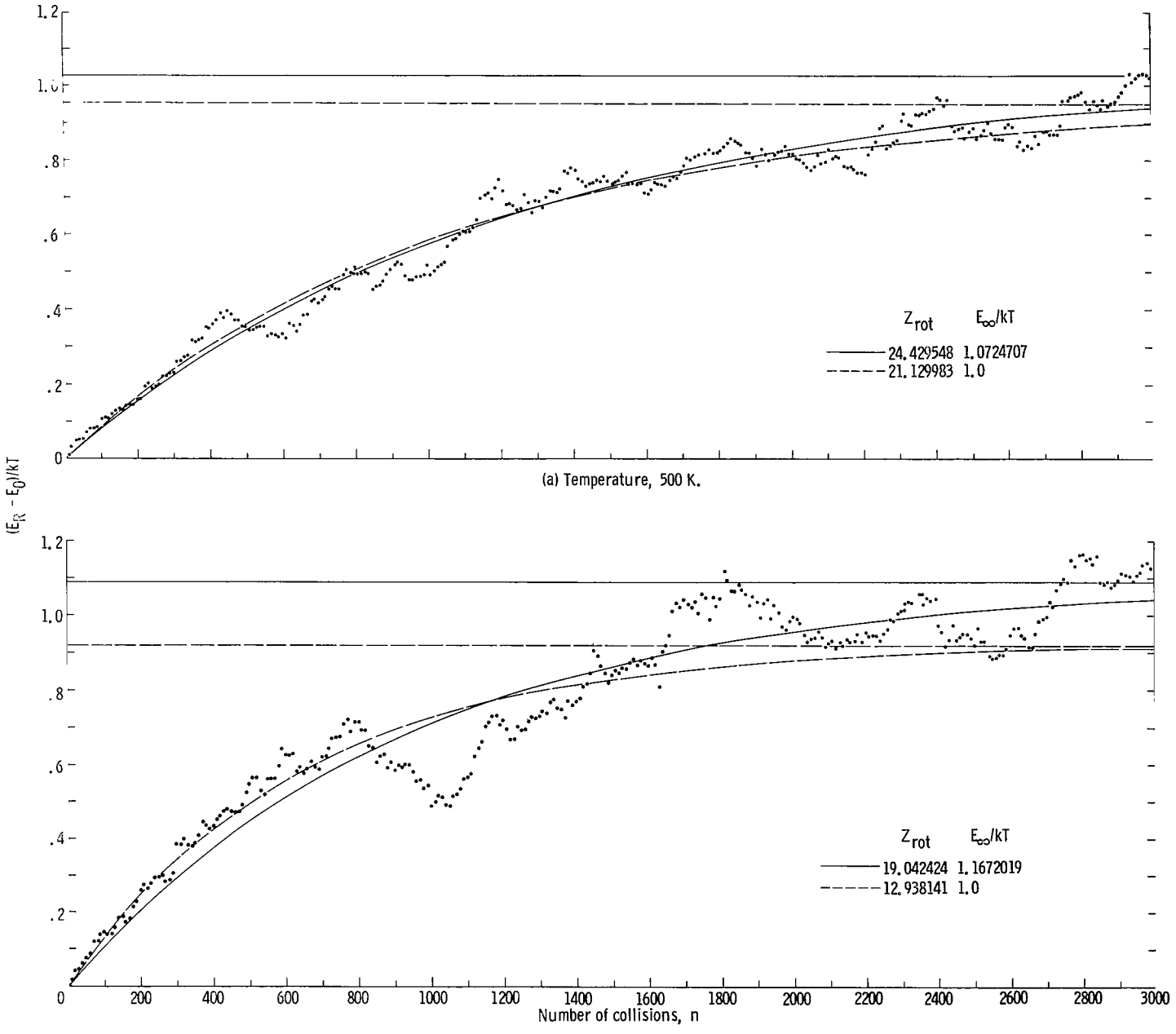

(a) Temperature, 500 K.

(b) Temperature, 300 K.

Figure 12. - Rotational relaxation of HCl.

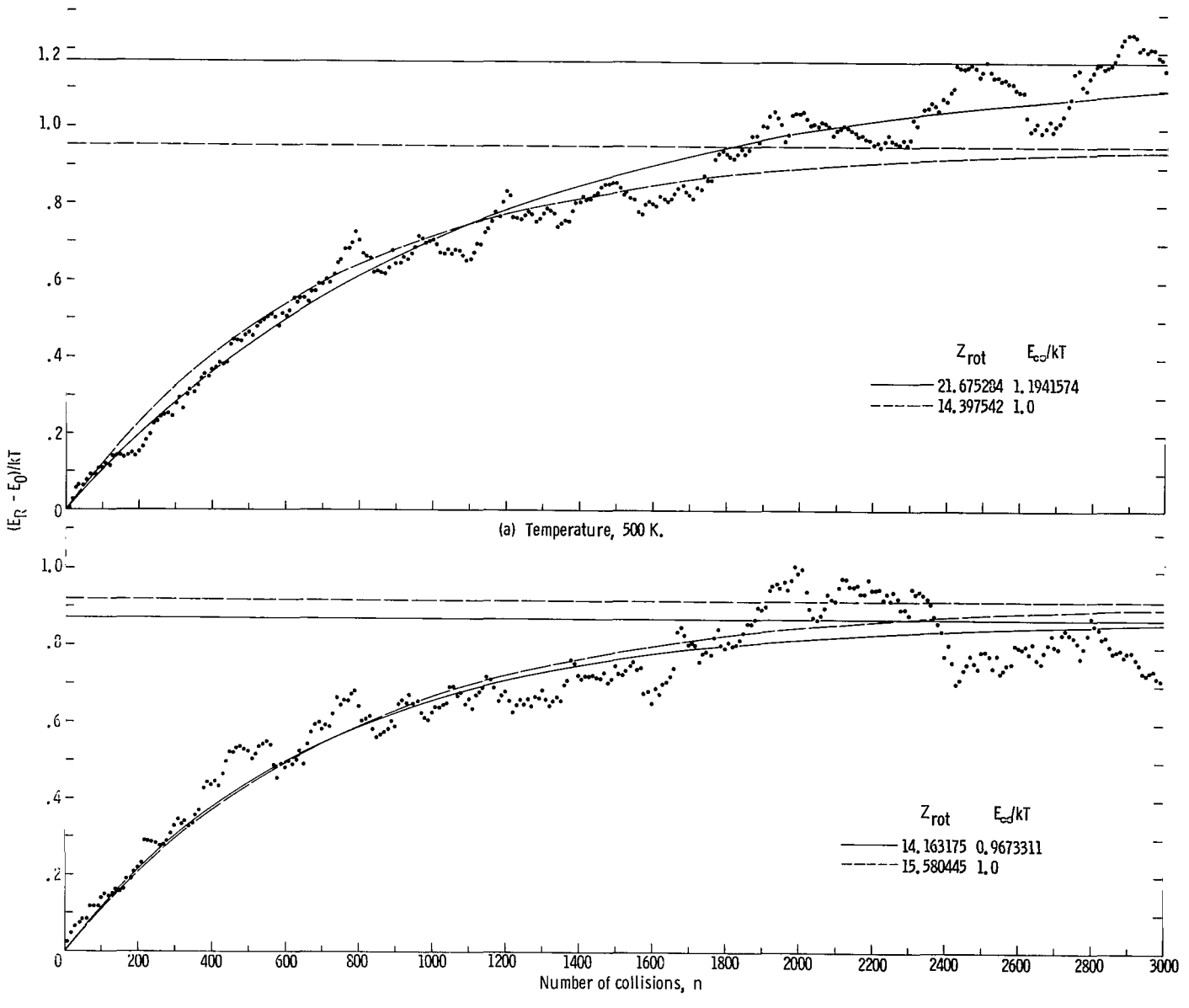

Figure 13. - Rotational relaxation of DCl.

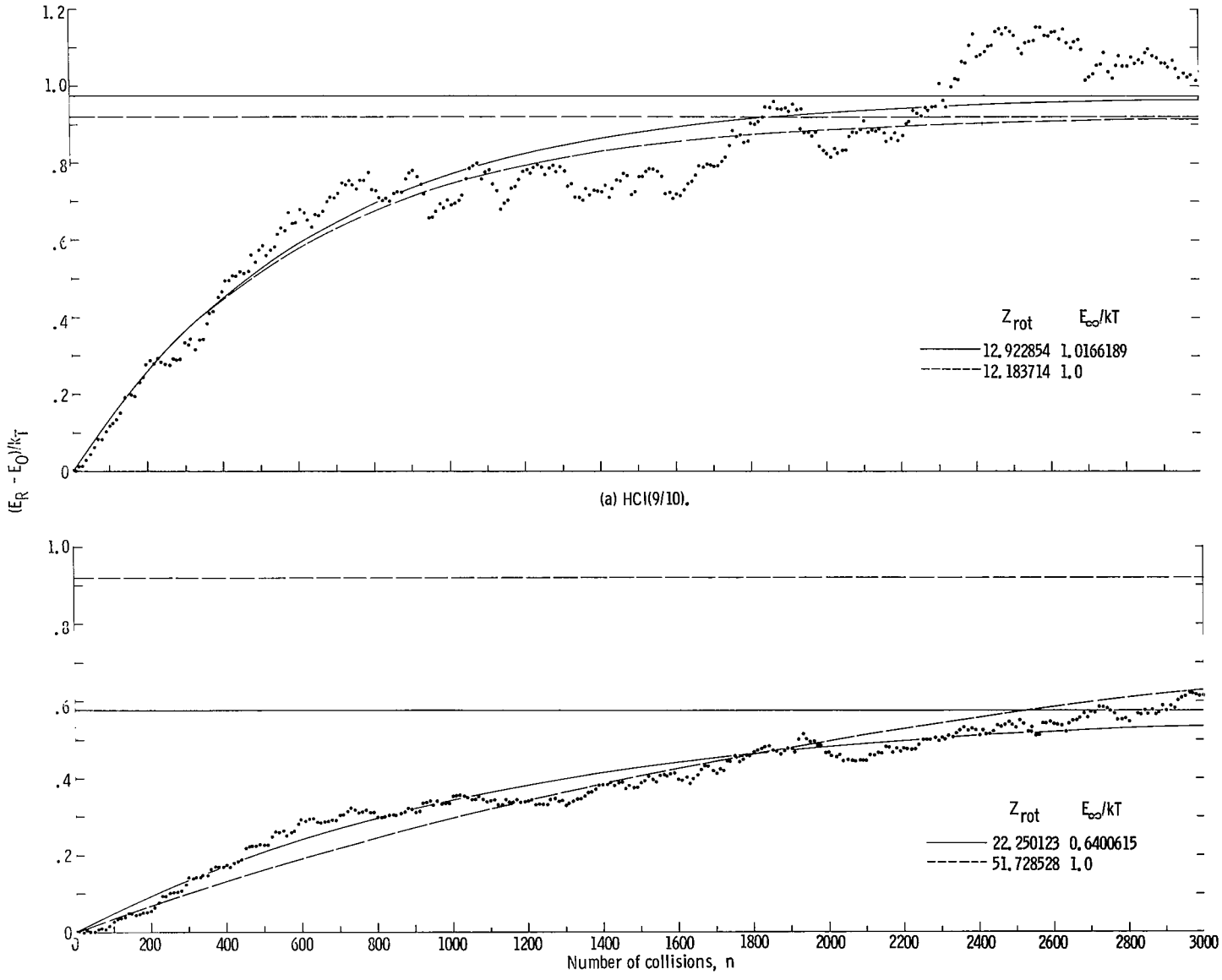

Figure 14. - Rotational relaxation of HCl(9/10) and HCl(1/2). Temperature, 300 K.

02U 001 49 51 3DS 71147 00903
AIR FORCE WEAPONS LABORATORY /WLOL/
KIRTLAND AFB, NEW MEXICO 87117

ATT E. LOU BOWMAN, CHIEF,TECH. LIBRARY

"The aeronautical and space activities of the United States shall be conducted so as to contribute . . . to the expansion of human knowledge of phenomena in the atmosphere and space. The Administration shall provide for the widest practicable and appropriate dissemination of information concerning its activities and the results thereof."

—NATIONAL AERONAUTICS AND SPACE ACT OF 1958

NASA SCIENTIFIC AND TECHNICAL PUBLICATIONS

TECHNICAL REPORTS: Scientific and technical information considered important, complete, and a lasting contribution to existing knowledge.

TECHNICAL NOTES: Information less broad in scope but nevertheless of importance as a contribution to existing knowledge.

TECHNICAL MEMORANDUMS: Information receiving limited distribution because of preliminary data, security classification, or other reasons.

CONTRACTOR REPORTS: Scientific and technical information generated under a NASA contract or grant and considered an important contribution to existing knowledge.

TECHNICAL TRANSLATIONS: Information published in a foreign language considered to merit NASA distribution in English.

SPECIAL PUBLICATIONS: Information derived from or of value to NASA activities. Publications include conference proceedings, monographs, data compilations, handbooks, sourcebooks, and special bibliographies.

TECHNOLOGY UTILIZATION PUBLICATIONS: Information on technology used by NASA that may be of particular interest in commercial and other non-aerospace applications. Publications include Tech Briefs, Technology Utilization Reports and Technology Surveys.

Details on the availability of these publications may be obtained from:

SCIENTIFIC AND TECHNICAL INFORMATION OFFICE

NATIONAL AERONAUTICS AND SPACE ADMINISTRATION

Washington, D.C. 20546